Journal of Volcanology and Geothermal Research 460 (2025) 108280

Contents lists available at ScienceDirect

Journal of Volcanology and Geothermal Research

journal homepage: www.journals.elsevier.com/journal-of-volcanology-and-geothermal-research

Chemical and isotopic characterization of groundwater and thermal waters from the Campi Flegrei caldera (southern Italy)

Stefano Caliro [a,*], Rosario Avino [a], Francesco Capecchiacci [a,b], Antonio Carandente [a], Giovanni Chiodini [a], Emilio Cuoco [a], Carmine Minopoli [a], Francesco Rufino [a], Alessandro Santi [a], Andrea L. Rizzo [c,d], Alessandro Aiuppa [e], Vincenzo Allocca [f], Pantaleone De Vita [f], Mauro A. Di Vito [a]

[a] Istituto Nazionale di Geofisica e Vulcanologia, Osservatorio Vesuviano, Napoli, Italy
[b] Dipartimento di Scienze della Terra, Università degli Studi di Firenze, Firenze, Italy
[c] Department of Earth and Environmental Sciences, University of Milano-Bicocca, Milano, Italy
[d] Istituto Nazionale di Geofisica e Vulcanologia, Sezione di Milano, Milano, Italy
[e] Dipartimento di Scienze della Terra e del Mare, Università di Palermo, Italy
[f] Department of Earth, Environmental and Resources Sciences, University of Naples Federico II, Naples 80126, Italy

ARTICLE INFO

Keywords:
Campi Flegrei caldera
Groundwater geochemistry
Hydrothermal systems
Volcanic aquifer degassing
Thermal waters
Carbon dioxide
Helium isotopes

ABSTRACT

We report here on the results of an extensive hydrogeochemical survey of the chemical and isotopic composition of thermal groundwater in the Campi Flegrei caldera (CFc), a restless volcanic system in the Campania Volcanic Province of Southern Italy. Our hydrogeochemical study, based on the collection of 114 groundwater samples, is the first comprehensive one since uplift, seismicity and degassing resumed in 2005, continuing today at accelerating rate. We use our results to characterize the processes that control the wide diversity of groundwater composition observed. We identify a set of key source processes governing the composition of the CFc thermal waters: i) the infiltration of meteoric water, responsible for the formation of diluted cold groundwater having bicarbonate as the prevalent anion (fresh waters), ii) mixing, upon downward infiltration in the aquifer(s), with high-temperature hydrothermal reservoir brines of probable marine origin (chloride waters), iii) the dissolution of a CO_2-He rich magmatic-hydrothermal gas, with isotopic signature (respectively $\delta^{13}C \sim -1$ ‰ vs. PDB and $^3He/^4He \sim 3Ra$, where Ra is the atmospheric He isotope ratio) similar to the Solfatara hydrothermal gases, generating bicarbonate-rich groundwater; (iv) near-surface dilution by hot condensates, formed by partial condensation of H_2S-rich Solfatara like hydrothermal steam, generating sulphate-rich steam heated waters. In near-surface environments, upward migrating groundwater also degases, releasing poorly soluble gas compounds (He, Ar, N_2, CH_4) and becoming enriched in more soluble CO_2. The above processes can work in concert, but each dominates in specific regions of the hydrothermal system, hence causing the extreme spatial diversity of water chemistry observed within the caldera. Our conceptual model for the processes acting within the thermal groundwater system will be crucial to interpreting any temporal change in groundwater chemistry observed in the installed permanent (instrumental) groundwater-monitoring network, which is critically needed for improving geochemical volcano monitoring during current acceleration of the unrest.

1. Introduction

Active volcanoes are sites of intense hydrothermal circulation, driven by mass/heat exchange between shallow infiltrated (meteoric/marine) waters and magmatic volatiles sourced by magma stored within the transcrustal magmatic plumbing system (Goff and Janik, 2000). These volcano-hosted hydrothermal systems are accessible to sampling at surface manifestations (springs, pools) or where tapped by wells. Because volcanic groundwater are so intimately related to processes taking place within the volcano engine, their chemical composition has long been used to monitor volcanic activity state, and to possibly identify hydrogeochemical precursors in the run-up to eruption (Martini,

* Corresponding author at: Istituto Nazionale di Geofisica e Vulcanologia, Osservatorio Vesuviano, via Diocleziano 328, Napoli, Italy.
E-mail address: stefano.caliro@ingv.it (S. Caliro).

https://doi.org/10.1016/j.jvolgeores.2025.108280
Received 14 September 2024; Received in revised form 16 January 2025; Accepted 22 January 2025
Available online 23 January 2025

1986; Martini et al., 1991; Shevenell and Goff, 1993; Bonfanti et al., 1996a, 1996b; Chiodini et al., 1996; Caliro et al., 1998, 1999, 2004; Delmelle et al., 1998; Sorey et al., 1998; Capasso et al., 1999; Valentino et al., 1999; Brombach et al., 2000; Goff et al., 2000; Lewicki et al., 2000; Varekamp et al., 2001; Tassi et al., 2003; Federico et al., 2004, 2023; Valentino and Stanzione, 2004; Evans et al., 2004; Lowenstern and Hurwitz, 2008; Rizzo et al., 2009, 2015; Hemmings et al., 2015; Jasim et al., 2015, 2018; Jasim, 2016; McCleskey et al., 2016).

The composition of volcanic groundwater is primarily controlled by the rates and mechanisms of gas-water-rock interaction within the aquifer (Giggenbach, 1988; Stimac et al., 2015). These in turn depend upon a variety of physical and chemical factors, which vary in both space (at the scale of the aquifer) and time. Spatial-temporal heterogeneities combine to produce very diverse environments of water-gas-rock interaction, causing the remarkable diversity of groundwater chemistry seen at volcanoes.

The Campi Flegrei caldera (CFc, Orsi et al., 2022 and references therein), in the densely inhabited metropolitan area of Naples (southern Italy), hosts a powerful hydrothermal system both in its submerged (the bay of Pozzuoli) and onshore sectors (Chiodini et al., 2022), with a number of especially vigorous surface manifestations (fumaroles, steaming and degassing soils/ground, and hot waters) concentrated within (and in proximity of) the Solfatara crater (Marini et al., 2022) (Fig. 1). The caldera is characterized by the "bradyseism" phenomena; literally, the term "bradyseism" derives from the Greek idiom and means "slow movement". It is widely used in the literature to identify the ground deformation occurring in the area of Pozzuoli village in the CFc, consisting in alternating phases of slow subsidence with generally more rapid uplift phases accompanied by low-magnitude earthquakes. The caldera entered a phase of unrest in the 1940s (Scarpa et al., 2022), with a further intensification in ground uplift and seismicity that took place during three bradyseismic crises in 1970–1972 (Corrado et al., 1977), 1982–1984 (Barberi et al., 1984) and 2005-present (Chiodini et al., 2016) motivated extensive research on hydrothermal fluid composition and flux (Cioni et al., 1984; Chiodini et al., 2001, 2003, 2016; Caliro et al., 2007, 2014). According to Caliro et al. (2007, 2014), the hydrothermal system is fed by a mixture of hot magmatic fluids (delivered by mafic magma stored at depth) and vapor generated by high temperature (~ 360 °C) vaporization of hydrothermal liquids of meteoric origin. This mixing zone is inferred to be located at the base of the hydrothermal system (at about 2 km depth), and to be overlain by a vapor-dominated plume centered underneath the Solfatara (Chiodini et al., 2022). Physical simulations (Chiodini et al., 2003, 2012, 2016) suggest that repeated pulses of magmatic gas injections into the hydrothermal system, caused by magma degassing episodes, are the likely driver of the unrest, and that these degassing episodes have increased in frequency (Chiodini et al., 2021, 2022) and injected mass of magmatic gases (Chiodini et al., 2016, 2021; Cardellini et al., 2017) during accelerating unrest since 2012.

As noted above, the chemical composition of groundwater is, at least in principle, an invaluable source of information to track episodes of escalating magmatic gas transport into the shallow hydrothermal system. However, no systematic characterization of groundwater chemistry has been attempted at CFc since acceleration of the unrest in 2012. Here, we report on the results of an extensive hydrogeochemical survey carried out in 2013–2014 to geochemically and isotopically (He, C, H and O isotopes) characterize the CFc groundwater system. Our aim here is to identify the main processes that control groundwater chemistry, and to derive hints into the source and fate of the released fluids.

2. The Campi Flegrei caldera (CFc)

The CFc is a long-lived resurgent caldera covering a large part of the coastal area west of Naples, Italy (Orsi et al., 1996, 2022). The present structure, comprising a 12 km wide caldera with other minor depressions, was largely determined by two main paroxysmal events, the

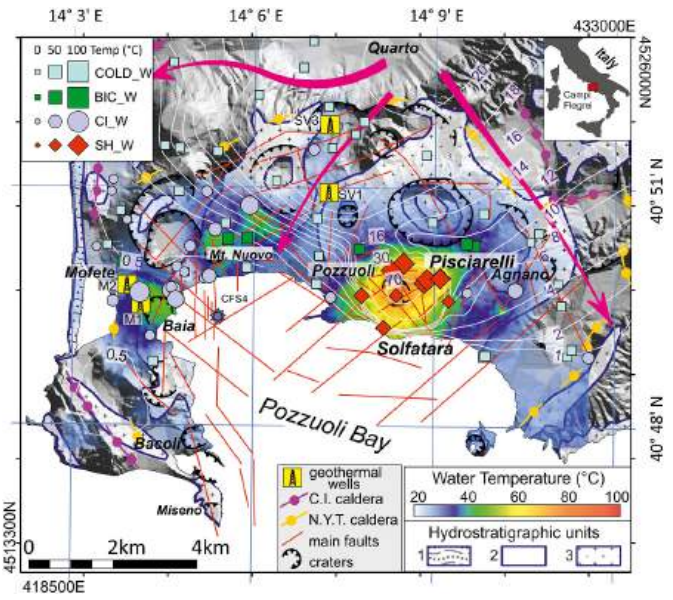

Fig. 1. Distribution of groundwater temperature based upon water samples collected in this work (sampling point locations shown), integrated with data from Aquater spa (1978), Aiuppa et al. (2006), Petrillo et al. (2013) and additional groundwater temperature measurements taken in the period from 2001 to 2018. Two main thermal clusters are present in the Solfatara-Pisciarelli and Baia Mofete areas. Contour lines are the water table surface and blue numbers indicate the piezometric level in meter a.s.l (Petrillo et al., 2013; De Vita et al., 2018). Magenta arrows indicate aquifer main preferential drainage. The elevated water table in Solfatara area is fed by fumarolic condensates. Red diamonds, steam-heated groundwater (SH_W); light blue squares, meteoric groundwater (COLD_W); green squares, bicarbonate-dominated thermal waters (BIC_W); grey circles, chlorine-dominated waters (Cl_W); purple star, submarine vents from the Fumose area (samples CFS4). Groundwater symbol dimensions are proportional to the water temperature. Geothermal wells: Mofete1 (M1), Mofete2 (M2), San Vito1 (SV1), San Vito3 (SV3). Campanian Ignimbrite caldera (C.I.); Neapolitan yellow tuff caldera (N.Y.T.); main faults and craters are modified after Selva et al. (2012) and Di Napoli et al. (2016). Hydrostratigraphic units: 1) alluvial-coastal complex formed by incoherent clastic deposits comprising all grain size classes, but with prevailing sandy terms. These deposits constitute heterogeneous and anisotropic porous aquifers. Groundwater flow can have hydraulic interchanges with freshwater bodies and/or with groundwater of the adjoining hydrogeological units; 2) ash-fall pyroclastic complex formed by incoherent deposits comprising lapilli and ashes, which, depending on different grain size classes, constitute heterogeneous and anisotropic porous aquifers with a generally low transmissivity; 3) ash-flow pyroclastic complex formed by ignimbrite deposits, from welded to scarcely welded, constituting anisotropic porous and fractured aquifers, generally characterized locally by a moderate transmissivity. Map of temperature was produced using the Sequential Gaussian Simulation algorithm (Deutsch and Journel, 1998). Coordinates are reported as geographic latitude and longitude and metric referring to the UTM projection (33 T zone), WGS84 datum. (For interpretation of the references to colour in this figure legend, the reader is referred to the web version of this article.)

Campanian Ignimbrite (39 ka BP) and Neapolitan Yellow Tuff (14 ka BP) eruptions (De Vivo et al., 1989; Orsi et al., 1992; Blockley et al., 2008). Over the last 14 ka, volcanic activity has occurred mainly within the caldera, commonly focused along its rim and regional faults (di Vito et al., 1999). After the last eruptive event (the Monte Nuovo eruption in 1538 A.D.; Di Vito et al., 2016), periodic episodes of unrest have occurred (Scarpa et al., 2022). Since the 1940s, CFc has been showing clear signs of potential reawaking, as revealed by recurrent episodes of ground uplift, shallow seismicity, and a visible increase in hydrothermal degassing (Del Gaudio et al., 2010; D'Auria et al., 2011; Chiodini et al., 2015). Two main uplift phases were recorded in 1970–1972 and in 1982–1984. In both cases, the deformation was confined within a radius

of 6 km, with maximum values registered at the center of the caldera of about 1.70 m and 1.80 m, respectively (Scarpa et al., 2022). The 1982–1984 bradyseism (Barberi et al., 1984) was followed by ~20 years of subsidence that terminated in November 2004, when ground uplift resumed, totaling about 1.3 m by the time of writing, and being accompanied by intense seismicity since 2018 (D'Auria et al., 2015; Chiodini et al., 2016; Bevilacqua et al., 2022; Kilburn et al., 2023; Giacomuzzi et al., 2024).

3. Hydrogeological background

The Campi Flegrei hydrothermal system has extensively been studied in the attempt to understand underground fluid circulation (Dall'Aglio et al., 1972; Celico et al., 1991; Rolandi and Stanzione, 1993; Tedesco et al., 1996) and the relations between bradyseismic events and groundwater chemistry (Ghiara and Stanzione, 1988; Martini et al., 1991; Celico et al., 1992; Tedesco, 1994).

The hydrogeological structure of the CFc is complicated by the presence of several overlapping lithotypes (e.g., tuffs, lava and sedimentary rocks) of variable thickness, grain-size distribution, porosity and permeability. The ultimate effect of this complex stratigraphy is the occurrence of different porous (unwelded pyroclastic deposits) and fractured (welded pyroclastic deposits and lavas) aquifers at shallow depths (Celico et al., 1987, 1991, 1992; Rosi and Sbrana, 1987; Allocca et al., 2018; Stellato et al., 2020; De Vita et al., 2018). Shallow groundwater circulation in the western and central sectors of the caldera defines an area with high piezometric levels, approximately 22 m a.s.l. in the Quarto area and ~ 70 m a.s.l. centered at the Solfatara area (Fig. 1) (e.g., Celico et al., 1991; De Vita et al., 2018), probably associated with deep fluid upwelling (Bruno et al., 2007). At the regional scale, a pseudo-radial groundwater flow pattern is defined by groundwater circulation towards the coastline in the southern, southeastern and western sectors, and towards the Campanian Plain aquifer in the northern sector (Celico et al., 1992; De Vita et al., 2018).

The bell shaped geometry of the water table in the Solfatara-Pisciarelli area (Fig. 1, Petrillo et al., 2013) is interpreted to be caused by the supply of steam condensates impacting the circulation and the chemical composition of groundwater in this area and surroundings.

Geothermal exploration wells drilled to about 3 km depth in the Mofete and San Vito areas (Fig. 1) have shed light into the deeper hydrothermal fluid circulation pathways (Guglielminetti, 1986; Rosi and Sbrana, 1987; De Vivo et al., 1989; Caprarelli et al., 1997), revealing the existence of a multi-reservoir geothermal system at depth (in the 550–2700 m depth range), characterized by high fluid salinities and temperatures (250–390 °C), and very diverse fluid origins (from primarily seawater-derived at <2000 m depth, to meteoric-magmatic in origin at >2000 m depth). These deep hot brines can locally rise through faults and fractures to mix with shallow groundwater (Aiuppa et al., 2006). These volcano-tectonic discontinuities also locally favor ascent and mixing between groundwater, deep and CO_2-rich mineralized fluids, and seawater.

4. Sampling and analytical methodologies

We report here on the composition of 114 water samples collected at CFc during May 2013 to March 2014. Samples are spatially distributed over an area of about 100 km^2 (Fig. 1). Values of pH, Eh, Electrical Conductivity (EC) and total alkalinity were determined directly in the field during sampling. Alkalinity was measured by acid titration with HCl 0.1 N on 100 ml of sample using methyl-orange as indicator. Water samples for chemical analyses were filtered with 0.45 μm filters and collected in 30 ml high-density polyethylene (HDPE) bottles. One aliquot was acidified with HCl 1:1 for the determination of cations. Samples were analyzed at the laboratory of fluid geochemistry at the INGV-Osservatorio Vesuviano, Naples. Major ions (Na^+, K^+, Mg^{2+}, Ca^{2+}, NH_4^+, Cl^-, NO_3^- and SO_4^{2-}) were determined by ion chromatography using a Dionex ICS3000 system. Dissolved gases (CO_2, N_2, O_2, Ar, CH_4, He) in water were analyzed following a modified method based on Chiodini (1996) and Caliro et al. (2008). Samples were collected in pre-evacuated ~200 ml glass vials equipped with a Teflon stopcock fixed with a rubber O-ring. In the field, the vial was filled with a volume of water, V_{liq} of about 2/3 of the total vial volume, V_{tot}. The gas phase separated in the headspace of the vial, of volume $V_{gas} = V_{tot}$-V_{liq}, was analyzed by a gas-chromatograph (HP 6890 N) through a unique injection on two analytical channels equipped with capillary columns (Molecular Sieve 5 Å 30 m × 0.53 mm × 50 μm and PLOT Q 30 m × 0.53 mm × 20 μm) and TCD detectors, using He as carrier gas on both channels. The partial pressure of each gas species (CO_2, N_2, O_2, Ar, CH_4) was determined referring to pure components at different pressures. Helium partial pressure in the head space of the vials was determined, on a second injection, by a leak detector (Alcatel ASM 142 - detection limit 0.00015 mbar). Based on partial pressure (P_i), the numbers of moles $n_{i,g}$ of each gas species contained in $V_{gas} + V_{inj}$ (where V_{inj} is the measured volume of the gas injection line) are calculated through the ideal gas law. After computing the partial pressures in the headspace of the vials ($p_{i,g} = (p_i{*}(V_{gas} + V_{inj}))/V_{gas}$), the number of moles of each gas species $n_{i,l}$ remaining in the liquid are calculated by means of the Henry's law (constants from Wilhelm et al., 1977), assuming that the gas phase separated in the headspace of the vial is in equilibrium with the liquid at laboratory temperature. The sum $n_{i,g} + n_{i,l}$ gives the total moles of each gas species in the water sample. The effect of salinity on gas solubility was not taken into account, as salinities of the examined solutions are relatively low.

For the determination of $\delta^{13}C$ of Total Dissolved Inorganic Carbon (TDIC), carbon species were precipitated in the field as $SrCO_3$ by adding $SrCl_2$ and NaOH as solid reactants directly in the sampling bottle. Carbonate precipitates were filtered and washed with CO_2-free distilled water under nitrogen atmosphere. Carbon isotope analyses were performed using a Finnigan Delta plus XP continuous flow mass spectrometer coupled with a Gasbench II device (analytical error $\delta^{13}C \pm 0.06$ ‰; data reported vs. V-PDB, Vienna Pee Dee Belemnite).

The oxygen and hydrogen isotopic composition of the collected waters was estimated by a near infrared laser analyzer (Picarro L2130i) using the wavelength-scanned cavity ring down spectroscopy technique (analytical errors: $\delta^2H \pm 0.5$ ‰, $\delta^{18}O \pm 0.08$ ‰; data reported vs. Vienna Standard Mean Ocean Water, V-SMOW).

The isotopic composition of He (as $^3He/^4He$) of the dissolved gas sample was determined at INGV-Sezione di Palermo, using a Helix SFT-GVI mass spectrometer for the isotopic measurements of helium and a Helix MC-Plus Thermo for ^{20}Ne, according to the method proposed by Inguaggiato and Rizzo (2004). Data are reported as R/R_a values (R_a is the He isotopic ratio in the atmosphere, as 1.39×10^{-6}; Ozima and Podosek, 2002), corrected for the atmospheric contamination using the sample $^4He/^{20}Ne$ ratio (Sano and Wakita, 1985).

The locations of sampling sites are reported in the map of Fig. 1, while the chemical and isotopic compositions of thermal waters are listed in Table S1.

5. Results

5.1. Physico-chemical parameters and major element composition

The sampled groundwaters are very diverse in terms of their physical parameters and chemistry of major ions (Table S1). Outlet temperature varies between 10.1 and 85.8 °C, pH from 1.54 to 8.9, electrical conductivity from 397 to 37,100 μS/cm, and total dissolved solids (TDS) from 93 to 34,200 mg/l (Table S1). About 60 % of the samples have pH less than 7, suggesting a pervasive interaction with volcanic/hydrothermal fluids rich in acidic volatiles (CO_2 and H_2S are major acidic species in the Solfatara fumaroles; Caliro et al., 2007). This is consistent with the widespread temperature anomaly that, while extending to the entire aquifer system, is particularly well visible in the Solfatara-

Pisciarelli area (Fig. 1). There, groundwater outlet temperatures of >60 °C are primary evidence for heating caused by the addition of hot fluids into the shallow aquifer. Electrical conductivity and TDS are broadly correlated with outlet temperature (Fig. 2 and Table S1). Cold groundwater ($T < 25$ °C) of likely meteoric origin typically contains less dissolved salts (< 1500 mg/l) than thermal waters, in which water-rock interaction is enhanced by higher temperatures, more intense rock leaching, and more powerful interaction with deeply sourced volcanic/hydrothermal fluids.

Diversity in groundwater chemistry is also illustrated in the Piper's diagram of Fig. 3, in which, as previously found (Valentino et al., 1999; Valentino and Stanzione, 2003, 2004; Aiuppa et al., 2006), three main water types can be identified: (1) bicarbonate-dominated groundwater, further separated into cold groundwater (COLD_W) and bicarbonate thermal waters (BIC_W) based on their temperatures and TDS (Fig. 2); (2) higher temperature (Fig. 2) chlorine-dominated groundwater (Cl_W); and (3) sulphate-dominated groundwater that, owing to their high temperatures (Fig. 2) and close proximity to the Solfatara-Pisciarelli fumarolic field (Fig. 1), are interpreted as steam-heated groundwater (SH_W; sensu Giggenbach, 1988) derived by the condensation of high-temperature, H_2S-rich hydrothermal steam (Aiuppa et al., 2006).

COLD_W are predominantly found along the peripheries of the caldera (Fig. 1) and, in addition to having low TDS (< 1500 mg/l) and temperatures (< 25 °C), are poor in alkalis (Fig. 4a, b) and have calcium as the main cation (Fig. 2). They are hence good proxies for the local meteoric recharge (Fig. 4). Cl_W, in contrast, are the most saline waters found at CFc (Fig. 2) and, being Na-K-rich, approach the composition of local seawater and the deep reservoir brines tapped by the Mofete geothermal wells (Fig. 4 a, b). Water samples (samples CFS4) collected in the submarine vents of the Fumose area (Di Napoli et al., 2016) exhibit similar alkalis-chlorine-rich compositions (Figs. 3–4). BIC_W have compositions intermediate between COLD_W and Cl_W (Fig. 4). Finally, SH_W are especially chlorine- and alkali-poor, confirming their mineralization is not controlled by mixing with either seawater or hydrothermal brines (as for the Cl_W), but rather by condensation of H_2S-rich fumarolic steam, followed by pervasive leaching of host rocks.

5.2. Oxygen and hydrogen isotopic composition

In previous work on oxygen and hydrogen isotopic compositions (Baldi et al., 1975; Valentino et al., 1999; Bolognesi et al., 1986), the CFc thermal waters have been interpreted as binary mixtures of local

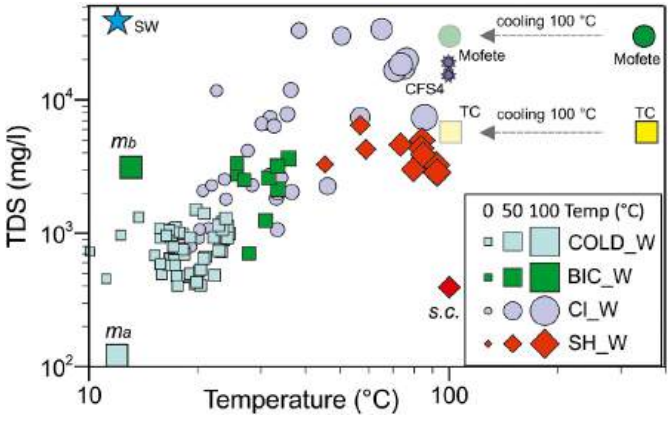

Fig. 2. Temperatures vs. total dissolved solids (TDS) scatter plot. Different symbols are used for the different water types, dimension of the symbols is proportional to the water temperature. Seawater and others endmembers (SW = seawater; m_a = meteoric low salinity; *mb* = meteoric bicarbonate; *sc* = steam condensate; Mofete = saline hydrothermal component; TC = low salinity hydrothermal component) are reported for comparison, see text for more details.

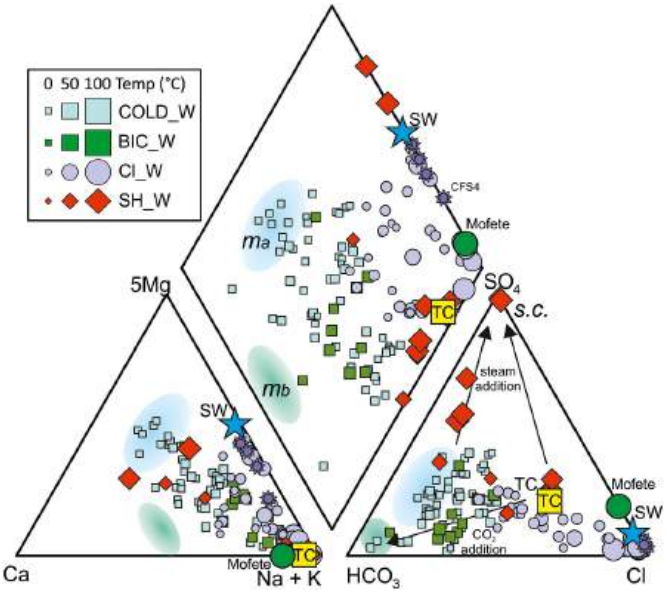

Fig. 3. Piper (1944) diagram. Symbols as in Fig. 2.

meteoric water ($\delta^{18}O$ -6.7 to −8 ‰ and $\delta^{2}H$ -33 to −42 ‰) and hot deep hydrothermal reservoir waters of marine origin ($\delta^{18}O$ + 1.2 ‰, $\delta^{2}H$ + 12 ‰). The recharge area of the meteoric component has been inferred to correspond to the carbonate massifs bordering the caldera, at a mean elevation of 370 m (Baldi et al., 1975).

Figure 5 illustrates our O and H isotopic results. In addition to the groundwater samples, we also plot the isotopic compositions of bulk steam condensates from the Solfatara fumaroles (Caliro et al., 2007), the calculated isotopic composition of liquids at equilibrium (at 100 °C) with the same Solfatara steam samples (we use liquid-vapor fractionation factors of $1000\ln\alpha_{(l\text{-}v)}$ (^{18}O) = 5.08 and $1000\ln\alpha_{(l\text{-}v)}$($^{2}H$) = 27.9, respectively, Horita and Wesolowski, 1994), the isotopic composition of local seawater, and the local meteoric water-line (Caliro et al., 1998).

Our CFc groundwaters exhibit an impressive isotopic variability, with δD and $\delta^{18}O$ compositions ranging from −46 to +22.3 ‰ and from −7.7 to +6.8 ‰ versus V-SMOW, respectively. $\delta^{2}H$ and $\delta^{18}O$ compositions are broadly positively correlated (Fig. 5a), identifying a linear trend with a slope of ~5, well below that of the meteoric water line. COLD_W and BIC_W plot above (or close to) the meteoric water line, confirming their meteoric derivation. In contrast, Cl_W, SH_W, and submarine vents (CFS samples) depart from the meteoric water line and point towards one (or more) isotopically heavy end-member component (s), lying somewhere between local seawater and the composition of the Mofete 1 hydrothermal brines (Fig. 5a). The most extreme isotopic compositions are observed for the Solfatara and Pisciarelli mud pools, whose extremely heavy $\delta^{2}H$ (> +10 ‰) and $\delta^{18}O$ (> +4 ‰) compositions suggest an input steam condensate and further non-equilibrium isotopic fractionation during boiling/evaporation at surface conditions (Giggenbach and Stewart, 1982). These processes of input of ^{2}H and $\delta^{18}O$ rich and Cl poor fumarolic steam condensate and surface boiling are depicted in Fig. 5b.

5.3. Dissolved gases

All groundwater samples contain gas species in dissolved form (Table S1). CO_2 is the dominant dissolved gas species in most samples (range, 0.005–33.8 mmol/l), followed by N_2 (0.04–1.12 mmol/l), O_2 (from b.d.l. to 0.4 mmol/l), and Ar (0.0006–0.03 mmol/l). CH_4 is observed at detectable levels (0.0002–0.22 mmol/l) in only 40 out of 112 samples, while He is observed at trace levels (2×10^{-6} - 0.0001 mmol/l) in all samples. Owing to the complex behavior of carbon in

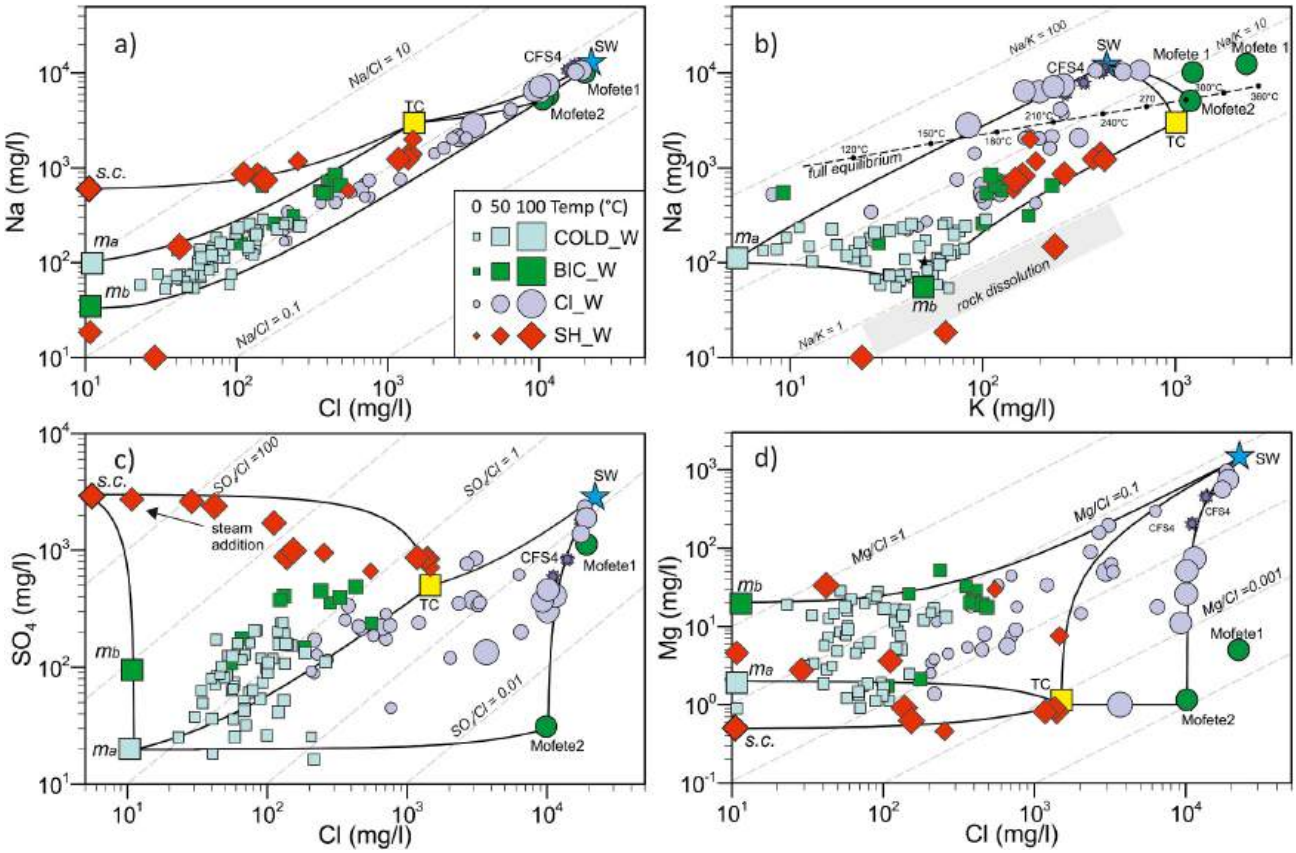

Fig. 4. Log-log scatter plots of major elements: a) Na vs. Cl; b) Na vs. K; c) SO_4 vs. Cl; d) Mg vs. Cl, of CF. Chemical composition of groundwater can be accounted for by mixing of different endmembers (see text), mixing lines are reported as black lines in the panels. In addition, panel b) reports the full equilibrium composition (Giggenbach, 1988), drawn assuming that Mg activity is controlled by the equilibrium with Mg-Chlorite in the temperature range of interest (Giggenbach et al., 1983), calculations were done by means of PHREEQC code (Parkhurst and Appelo, 1999). Note the relatively high Na and K concentrations of the "fully equilibrated" water.

aqueous solutions (see discussion), we use Total Dissolved Inorganic Carbon (instead of the CO_2 concentration) as a better proxy to fully characterize the carbonate system.

Carbon concentration (TDIC) and N_2 are broadly negative correlated (Fig. 6a), implying diverse sources. High TDIC concentrations are in general characterized by high pCO_2 values and are associated with low N_2 and Ar concentrations (Table S1). This behavior suggests that the addition of a deep CO_2 rich gas phase leads to an increase in the total pressure of dissolved gases, and causes degassing upon ascent/decompression, indicating a barometric control on the composition of the dissolved gases. The most N_2-rich samples are the meteoric-derived (Fig. 5) COLD_W, suggesting atmospheric derivation of this gas. This is corroborated by the positive correlation between N_2 and Ar (Fig. 6b), with most COLD_W exhibiting N_2/Ar of ~40, close to that of air-saturated water at 0–20 °C and 0–1200 m (the supposed meteoric water infiltration temperature and elevation, based on the height of carbonate massifs boarding the Campanian Plain). Samples with N_2/Ar ratios of ~83 reflect air contamination upon (or prior to) sampling. Oxygen, the second most abundant component in air, is high in many N_2-rich groundwaters (Table S1), but the weak N_2-O_2 correlation (not shown) reflects its non-conservative behavior upon infiltration and groundwater discharge (O_2 is typically consumed by redox reactions in aquifers; at CFc, this is testified by recurrent reducing redox conditions, with measured redox potentials (E_H) as a low as −241 mV). Thermal waters (BIC_W, Cl_W, and SH_W) are to a variable extent depleted in air components and enriched in CO_2, with the most CO_2-rich samples corresponding to BIC_W. In the thermal waters, CO_2 levels are well in excess of those characteristic of air saturated groundwater, requiring an additional, non-atmospheric source.

5.4. He and C isotopes

Helium has very contrasting $^3He/^4He$ signatures, having R/Ra =1 in air, R/Ra ~0.02 in the continental crust (Ozima and Podosek, 2002), and in the Earth's mantle R/Ra > > 1 (with MORB range at 8 ± 1 Ra; Graham, 2002). Thus, this ratio is a very useful tracer to resolve atmospheric vs. endogenous (magmatic, mantle, or crustal) sources of fluids in volcanic groundwater (Sano and Fischer, 2013). Dissolved He in the CFc groundwater samples is isotopically heterogeneous, ranging from 0.089 to 2.73 R/Ra and a Ne/He from 0.17 to 13.1, with the highest R/Ra values approaching the isotopic compositions of the Solfatara fumaroles.

Figure 7 plots the He isotope compositions of our groundwater samples vs. (a) the Ne/He ratio and (b) the N_2/He ratio. These chemical ratios between inert/unreactive components are suitably combined with He isotopes because they are orders of magnitude higher in air than in the crust/mantle (Fig. 7). We find a broad negative correlation between R/Ra and Ne/He-N_2/He ratios (Fig. 7), indicating that the data variability is predominantly controlled by mixing between an atmospheric component (air, and/or air-saturated groundwater) and a Solfatara-like hydrothermal gas. However, a number of groundwater samples have R/Ra composition well below 1, and trend towards a possible crustal endmember characterized by R/Ra ~ 0.02, a Ne/He ratio 0.001 and N_2/He ratio of 1.000, compatible with a radiogenic crustal source (Sano and Wakita, 1985). These endmembers are estimated by fitting samples compositions with simple mixing models as depicted in Fig. 7. In

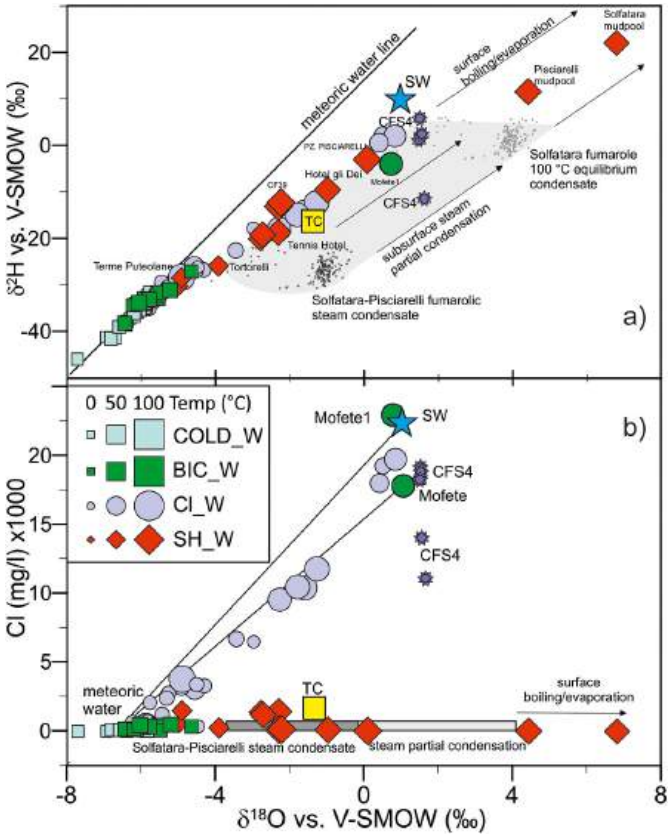

Fig. 5. Chemical-isotopic diagrams of CF groundwater: a) $\delta^{18}O$ vs. $\delta^{2}H$ and b) $\delta^{18}O$ vs. Cl. Composition of steam discharged by the Solfatara vents, of seawater, of submarine thermal water CFS4 (Di Napoli et al., 2016), the meteoric water-line (Caliro et al., 1998) and the composition of the equilibrium liquid phase condensed from steam of Solfatara vents at 100 °C are also reported.

particular, most of the samples indicate that all the three endmembers are concurrently involved in defining the dissolved gas compositions. The fractions of each endmember can be derived from the following equations (modified from Sano and Wakita, 1985):

$$\left({}^{3}He/{}^{4}He\right) = \left({}^{3}He/{}^{4}He\right)_{a} \times fA + \left({}^{3}He/{}^{4}He\right)_{h} \times fH + \left({}^{3}He/{}^{4}He\right)_{r} \times fR \quad (1)$$

$$\left({}^{20}Ne/{}^{4}He\right) = \left({}^{20}Ne/{}^{4}He\right)_{a} \times fA + \left({}^{20}Ne/{}^{4}He\right)_{h} \times fH + \left({}^{20}Ne/{}^{4}He\right)_{r} \times fR \quad (2)$$

$$1 = fA + fH + fR \quad (3)$$

where the subscripts *a*, *h*, and *r* refer to the asw, hydrothermal and radiogenic (crustal) endmembers, respectively. The computed correspondent fractions *fA*, *fH* and *fR* are reported in Table S1.

A similar approach can be apply to derive endmember fractions by considering nitrogen concentrations. Accordingly, eqs. 1 and 3 remain the same while eq. 2 can be written as:

$$\left(N_2/{}^{4}He\right) = \left(N_2/{}^{4}He\right)_{a} \times fA + \left(N_2/{}^{4}He\right)_{h} \times fH + \left(N_2/{}^{4}He\right)_{r} \times fR \quad (4)$$

Figure 7a and b also report the mixing lines computed for fractions of hydrothermal component *(fH) of* 10 %, 50 % and 90 %.

The carbon isotope composition ($\delta^{13}C$) of Total Dissolved Inorganic Carbon (TDIC) varies from −17.1 ‰ to +2.34 ‰ (Table S1). The meteoric-derived COLD_W exhibits the lightest (most negative) $\delta^{13}C$ values (−17.3 to −5.1 ‰), reflecting a primary biogenic origin of TDIC (2.2–14.5 mmol/l) (Fig. 8). Thermal waters (BIC_W, Cl_W, and SH_W)

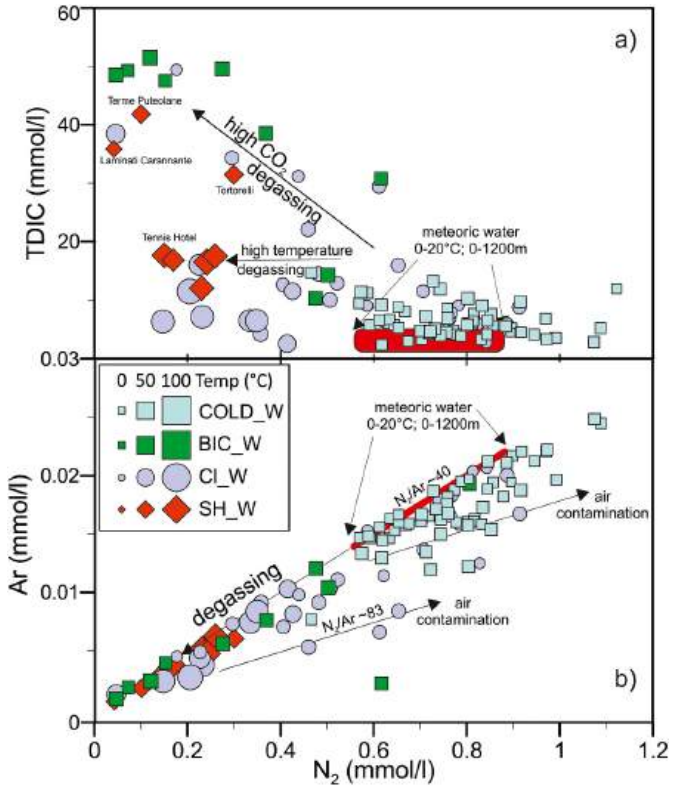

Fig. 6. Dissolved gases in CF groundwater: a) N_2 vs. TDIC and b) N_2 vs. Ar. Depletion in atmospheric components is accompanied by an increase of TDIC (CO_2) and/or induced by the increased temperature of groundwater. The addition of a CO_2 rich gas phase leads to an increase in the total pressure of dissolved gases, and causes degassing upon ascent/decompression, suggesting barometric control on the composition of the dissolved gases.

are increasingly enriched in an isotopically heavy carbon component. For reference, the characteristic $\delta^{13}C$ composition of the Solfatara fumaroles is −1.3 ± 0.4 ‰ (Caliro et al., 2014).

6. Discussion

In regions of active volcanism, groundwater stands at the interface between the shallow meteoric system and the underlying magmatic-hydrothermal system. As such, groundwater composition reflects a dynamic balance resulting from fluid contributions from both surface (atmosphere/biosphere/seawater) and deeper (crustal rocks, magmas, and their mantle sources) environments (Jasim et al., 2018). The complex interactions that result cause volcanic groundwater to vary widely in both space (at the scale of a given volcanic aquifer) and time, a fact that can potentially be exploited to monitor volcanic activity state when/if the volcano becomes restless (e.g., Cronan et al., 1997). For volcanic groundwaters to be useful for volcano monitoring, however, a thorough understanding of the processes that control their chemistry is required. This is today especially relevant at CFc, in view of the ongoing deformation/seismic/degassing unrest beginning in the early 2000s (Chiodini et al., 2003, 2016, 2021) and that continues at an accelerating rate (Kilburn et al., 2017, 2023; Bevilacqua et al., 2022) at the time of this writing. Here we use the results of our comprehensive 2013–2014 hydrogeochemical survey, the first since the bradyseismic crisis, to analyze the key processes controlling groundwater chemistry at CFc.

6.1. Steam condensation

Perhaps the most striking aspect of our dataset is the prominent groundwater temperature anomaly in the Solfatara-Pisciarelli district

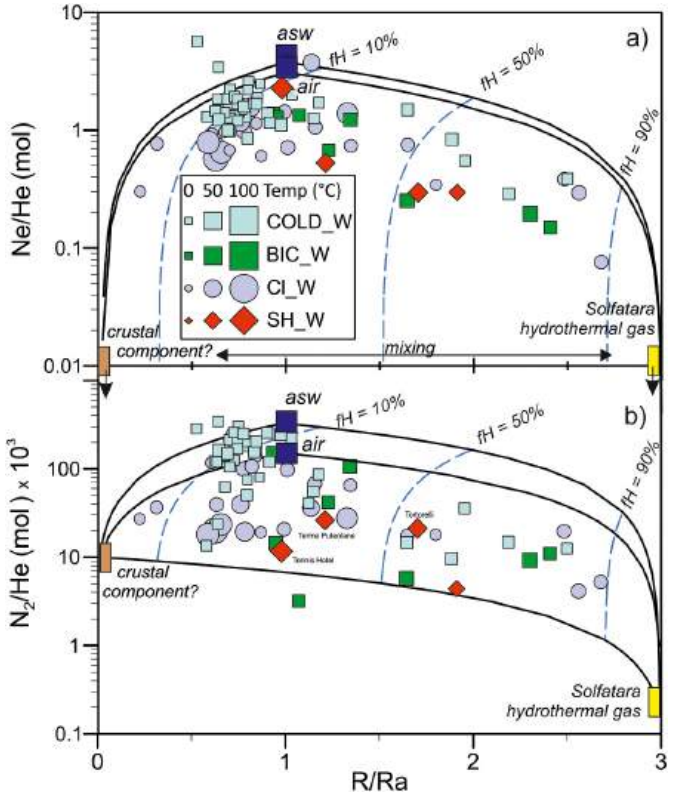

Fig. 7. He isotope composition (R/Ra) of CFc groundwater samples, plotted versus (a) Ne/He and (b) N_2/He ratios. The mixing lines between different end-members are shown, along with the mixing lines computed for 10 %, 50 % and 90 % fractions of the hydrothermal components (*fH*) (see text).

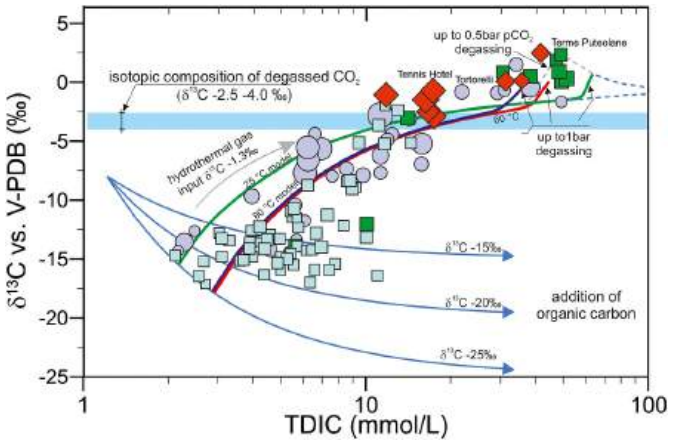

Fig. 8. $\delta^{13}C_{TDIC}$ vs. TDIC scatter plot of CFc groundwater. Samples exhibit a general trend from low TDIC and ^{13}C-depleted compositions towards high TDIC and more positive $\delta^{13}C$ compositions. The figure also shows the model evolution of groundwater as calculated by numerical simulations: blue lines, obtained by adding to a meteoric water (with a TDIC of ~1 mmol/L and $\delta^{13}C$ of −8 ‰) a CO_2 with biologic signature from $\delta^{13}C$ -25 ‰ to −15 ‰. The input of biologic carbon during the infiltration is evident for the bicarbonate cold water. Green, red and purple lines: starting from the results of the previous models, three simulations are carried out at different temperatures (25–60-80 °C) by adding 0.1 mol of a hydrothermal Solfatara-like gas phase in 100 steps, allowing the solution to degas at 1 bar of total gas pressure. Degassing lines at 0.5 bar of pCO_2 are also reported as grey shaded lines.

(Fig. 1). The Solfatara crater is a maar-like, sub-hexagonal depression, bounded by steep faults, formed by repeated explosive (phreatic to phreatomagmatic) activity during the most recent epoch (epoch III) of volcanic activity at Campi Flegrei, at ca. 4200 yr B.P. (Isaia et al., 2015). With the adjacent Pisciarelli fumarolic system (Isaia et al., 2021), the Solfatara crater has historically been the largest hydrothermal manifestation in the CFc (Guidoboni and Ciuccarelli, 2011; Marini et al., 2022). Recently, hydrothermal activity from fumarolic vents, boiling mud pools, and steaming grounds/soils has significantly increased during the 1982–1984 (Orsi et al., 1999) and 2005-present (Chiodini et al., 2016, 2022) unrest. Because of this especially intense hydrothermal degassing activity, and based on geophysical (Isaia et al., 2015) and geochemical (Caliro et al., 2014) evidence, the Solfatara volcano has been interpreted (Chiodini et al., 2022) as the surface outflow zone of a vertically extended (from the base of the hydrothermal system at ~2–3 km depth to about 300–500 m depth) "gas plume", formed by complete vaporization of hydrothermal brines by magma-sourced volatiles. Steam transported in this gas plume would condense in the near-surface (at 300–500 m depth), where electrical resistivity tomography (Byrdina et al., 2014; Troiano et al., 2014; Gresse et al., 2017) and audio-magneto-telluric (Siniscalchi et al., 2019) results indicate the presence of very conductive layer(s). According to Chiodini et al. (2001), condensation of not less than 3000 tons/day of steam would result in a heat energy transfer of about $7.5{\cdot}10^{12}$ J/d. Steam condensates, supplied at a rate of about 40–50 L/s, are thought to feed the local aquifer, inducing the bell-shaped geometry of the water table in the Solfatara-Pisciarelli area (Fig. 9, Petrillo et al., 2013) and impacting the chemical and isotopic composition of groundwater in this area and surroundings. In light of the above, we interpret the temperature anomaly in the Solfatara-Pisciarelli district (Figs. 1, 9) to be (primarily) caused by heat generated by this steam condensation process.

Chemically, hydrothermal steam condensation is known to generate SO_4-dominated steam-heated groundwater, in which dissolved sulphate is produced by aqueous-phase oxidation of hydrothermal H_2S (Giggenbach, 1988). At CFc, the clustering of SH_W groundwater in the Solfatara-Pisciarelli area, with high SO_4/Cl ratios (Fig. 10a), supports the prominent role of steam condensation in this area.

Steam condensation in the shallow aquifer is additionally strongly supported by O—H isotopic results (Fig. 5). Simple mixing between (i)

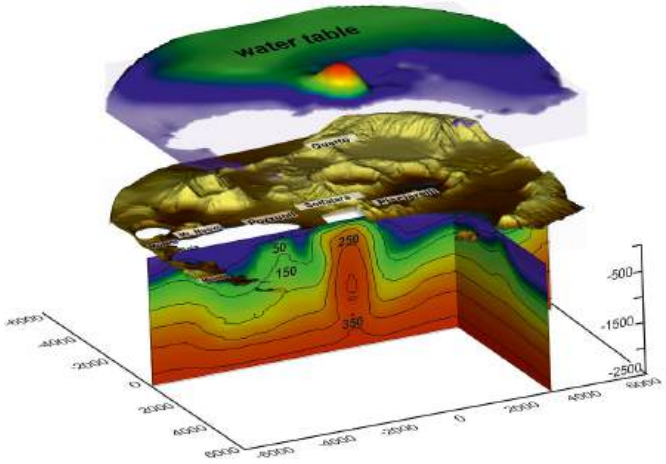

Fig. 9. 3D view of the water table morphology. This exhibits a bell-shaped geometry centered at Solfatara caused by steam condensation of hydrothermal fluids. The vertical section refers to temperatures (°C) resulting from the 3D physical model of the Campi Flegrei geothermal system developed by using the TOUGH2 code simulator (for details see Petrillo et al., 2013).

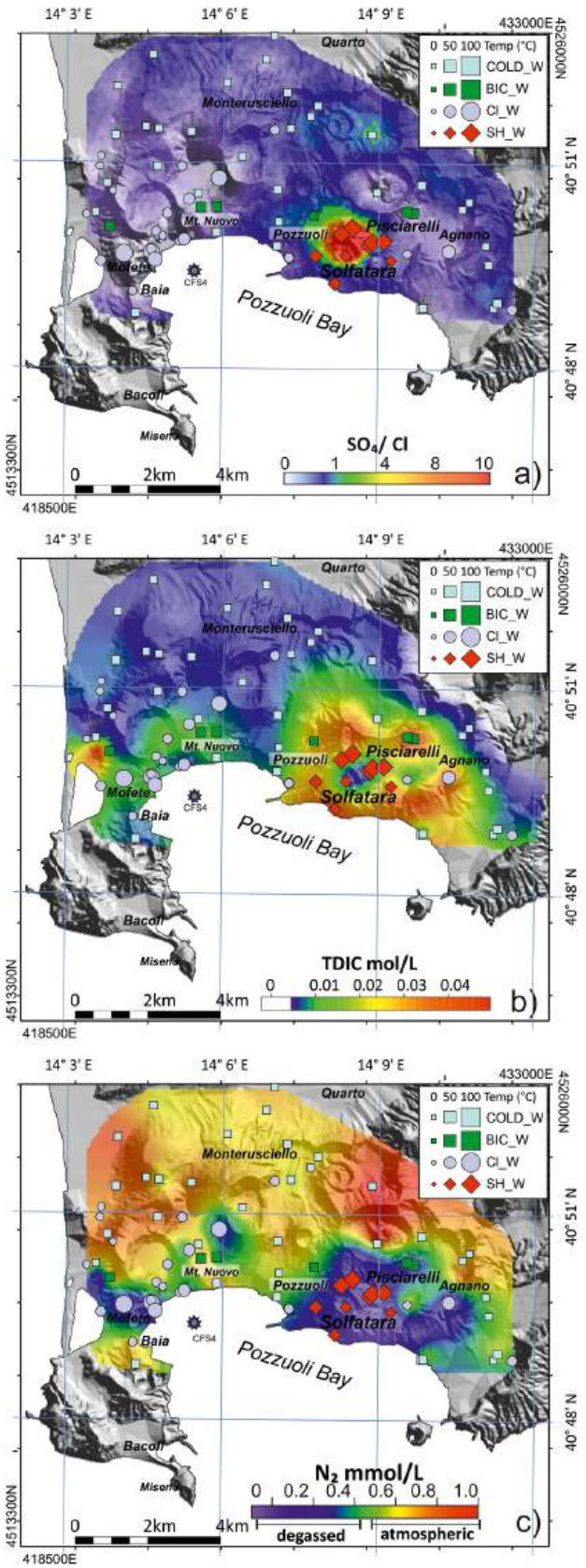

Fig. 10. Maps of (a) SO_4/Cl ratio in CFc groundwater; (b) total dissolved inorganic carbon (TDIC) concentration in CFc groundwater; and c) the dissolved nitrogen concentration in CFc groundwater.

meteoric water and (ii) seawater and/or hydrothermally modified seawater, as preliminarily indicated by Fig. 5a and as suggested in earlier studies (Baldi et al., 1975; Valentino et al., 1999; Bolognesi et al., 1986), is inconsistent with the Cl vs. $\delta^{18}O$ systematics (Fig. 5b), in which two divergent data trends are observed. In this diagram, the Cl_W are indeed well explained by variable extents of dilution (by meteoric water) of hydrothermally processed seawater (Mofete 1) or pure seawater; however, the SH_W (and to some minor extent the BIC_W) align along a nearly horizontal trend that requires an isotopically heavy component that carries essentially zero chlorine. Liquids formed by partial condensation of a Solfatara-Pisciarelli fumarolic steam (Cl ~ 5 ppm; calculated $\delta^{18}O$ values of ~0 to +4 ‰) manifest these characteristics. The Fumose submarine vents (CFS samples) plot in an intermediate position between the two trends (Fig. 5b), indicating they experience both (i) mixing with hydrothermal brines/seawater and (ii) steam heating.

6.2. Mixing

Volcano-hosted groundwater systems in general (Jasim, 2016), and the CFc thermal groundwater system in particular (Celico et al., 1992; Rolandi and Stanzione, 1993), are complex sequences of superimposed aquifers, hosted in lithologically distinct geological units of different mineralogy/porosity/permeability. Each of these water bodies then evolves its own specific chemical flavor from the peculiar temperature regime, gas-water-rock reaction environment, and meteoric/seawater vs. deep fluid supply. However, geological discontinuities such as faults and fractures locally favor mixing between these distinct water bodies, generating groundwater of hybrid chemistry. Saline hot brines can locally rise to mixed with shallow meteoric-dominated groundwater (Aiuppa et al., 2006), as in the case of CFc (Guglielminetti, 1986; Rosi and Sbrana, 1987; De Vivo et al., 1989; Caprarelli et al., 1997). In the Mofete area (Fig. 1) for example, exploratory geothermal drilling in the 1970s–1980s revealed the existence of three distinct superimposed hot aquifers at depths of 500–900 m (temperatures of 210–250 °C), 1800–2000 m (temperatures of 295–310 °C), and 2500–2700 m (temperatures of 340–360 °C) (Guglielminetti, 1986; see also references in Marini et al., 2022). Upon ascent, these hot reservoir brines can act as sources of dissolved components to shallow thermal groundwater.

Figure 4 explores the mixing relationships between the different water types at CFc using major elements. From this analysis, we propose that a large part of the observed groundwater chemical diversity can be accounted for by mixing – in various proportions – of 6 distinct end-members (compositions listed in Table 1):

i. local seawater (SW);
ii. two low-salinity (m_a, m_b Cl ~ 10 mg/l) endmembers, representing variably mineralized (see their different Na, K and Mg contents) infiltrated meteoric water (see their meteoric O and H isotopic signature; Fig. 5);
iii. a Cl-poor (~5 mg/l) and SO_4-rich (~3000 mg/l) component, interpreted as a hydrothermal steam condensate (*s.c.*) (cfr. 6.1);
iv. a hot/saline hydrothermal brine component (Fig. 2), here represented by the composition of the Mofete 2 drilling fluids (Cl ~10,000 mg/L) that, from O and H isotopic evidence, can be

Table 1
Chemical composition of potential end-members involved in the mixing processes affecting of CF groundwaters. Concentrations are reported in mg/L.

	Na	Cl	Mg	K	SO4
Mofete2	5090	10,200	1	1200	30
SW	12,250	22,390	1397	440	2900
m_a COLD_W	100	10	2	5	20
m_b BIC_W	35	10	20	50	20
s.c.	600	10	0.5	1	3000
TC	3000	1500	1	1000	500

interpreted as infiltrated seawater modified by some Solfatara-like steam addition (Fig. 5) and water-rock interaction (as indicated by the manifest Mg and SO_4 depletions relative to seawater; Fig. 4);

v. a less saline (Fig. 2) hydrothermal component (TC, Cl ~ 1500–2000 mg/L), equilibrated at high temperature (~350 °C, Fig. 11), discharged in the Pisciarelli area, mostly represented by the Tennis Hotel sample. From chemical and isotopic point of view, this thermal component can be interpreted as an original mixture of hydrothermal brine (e.g, the liquid encountered in the local CF23 geothermal well; Caliro et al., 2007) with steam condensates.

The relative contributions of the 6 endmembers described above are different in the various water types identified. In particular, Cl_W are interpreted to reflect mixing between endmembers local seawater (SW), Mofete brines and meteoric waters (m_a and m_b); while SH_W are dominated by end-member *s.c.*, but also receive contributions from the *TC* hydrothermal component and meteoric water (m_a and m_b). These different water types also evolve in distinct thermal regimes, as indicated by comparison with the theoretical compositions of fully equilibrated fluids with reservoir rocks (Giggenbach, 1988, Fig. 11). Plotting our results in Giggenbach's (1988) triangular plot highlights that Cl_W reflect equilibrium conditions with the host rocks at ~140–160 °C (well below the Mofete reservoir fluids equilibrated at ~320 °C), while SH_W fall in the field of immature and/or partially equilibrated waters, with the most Na-rich samples potentially indicating deep equilibrium temperatures in the source reservoir (the TC thermal component perhaps?) at 240 to 340 °C (Fig. 11). This behavior could support the existence and mixing of the distinct superimposed hot aquifers found in the Mofete area (Fig. 1) from the exploratory geothermal drillings carried out in the 1970s–1980s (Guglielminetti, 1986; see also references in Marini et al., 2022).

6.3. Ingassing and degassing

The infiltrated meteoric waters (COLD_W) that recharge the shallow CFc aquifer system contain a dissolved gas phase of atmospheric origin, as indicated by their high N_2 and Ar concentrations, and N_2/Ar ratios close to air or air-saturated groundwater (Fig. 6). However, as these recharge waters enter the core of the hydrothermal system (the inner central portion of the caldera; Fig. 1), they increasingly interact with a deeply sourced, CO_2-rich magmatic-hydrothermal vapor phase (Fig. 10b, c). The N_2 vs. TDIC (CO_2) plot (Fig. 6a) demonstrates this clearly, showing that BIC_W exhibit an especially steep negative dependence that implies progressive replacement of atmospheric gases by a CO_2-rich magmatic-hydrothermal phase (Fig. 10b). The Cl_W and SH_W waters exhibit less steep relationships, e.g., more modest CO_2 increases, indicating dilution by condensed steam in the main hot outflow zone of the Solfatara "gas plume" (see the CO_2 relative low in the hot core of the hydrothermal system; compare Fig. 10a and b).

The progressive dissolution of deeply sourced magmatic-hydrothermal volatiles is especially well tracked by He (Fig. 7) and C (Fig. 8) isotopes. The CFc groundwaters are variably enriched in non-atmospheric He, as indicated by their below-air Ne/He (from 0.17 to 13.1) and N_2/He ratios, and R/Ra ratios $\neq 1$ (Fig. 7). Considering the observed spread of isotope compositions (0.089 to 2.73 R/Ra), we interpret the excess (non-atmospheric) He in our thermal groundwater samples to reflect mixing between (i) a magma-sourced fluid whose He isotope composition is constrained by Solfatara fumaroles, 2.85 ± 0.12 Ra (Caliro et al., 2014); this range of values agrees with measurements in off-shore gas discharges from the Pozzuoli Bay (0.9–3.1 Ra; Tedesco et al., 1990; Vaselli et al., 2011) and fluid inclusions in olivines and clinopyroxenes from mafic volcanic rocks (2.5–3.0 Ra; Martelli et al., 2004) and (ii) a crustal component with R/Ra < 0.1, perhaps deriving from re-mobilization of radiogenic He ingrowth in the crustal basement. This crustal component is also evident in the TDIC-^{3}He-^{4}He triangular plot of Fig. 12.

The same plot also shows that the CFc thermal groundwater samples are enriched in CO_2 relative to He compared to a "magmatic" end-member exemplified by the Solfatara fumarolic gas. Since CO_2 is more soluble in water than He (Ballentine et al., 2002), selective/preferential He loss upon water decompression and degassing during groundwater ascent (to surface discharge at atmospheric pressure) can explain the CO_2/He mismatch between groundwater and fumaroles. It is also possible, however, that some of the excess CO_2 derives from remobilization of hydrothermal calcite, as recently proposed (Chiodini et al., 2015; Buono et al., 2023).

The overall message recorded by dissolved gases is hence that of a

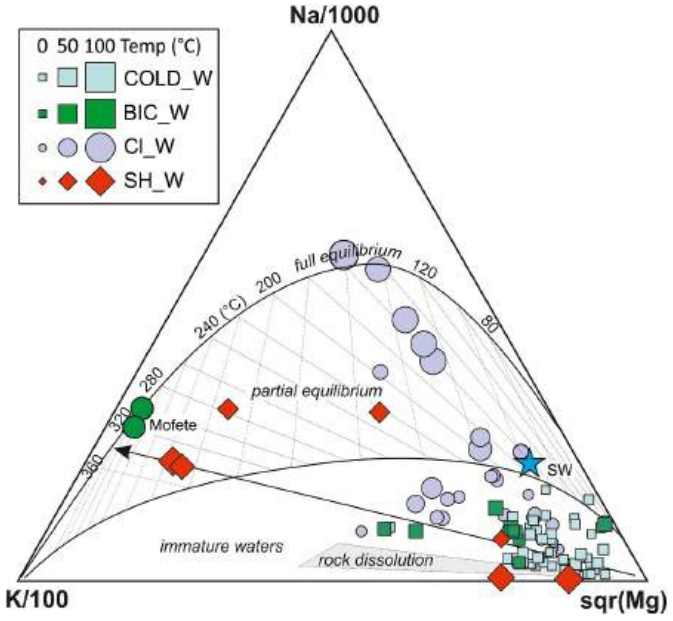

Fig. 11. Ternary Na-K-Mg geothermometric diagram (modified from Giggenbach, 1988). Temperatures as high as 340 °C are estimated for samples discharged at Pisciarelli.

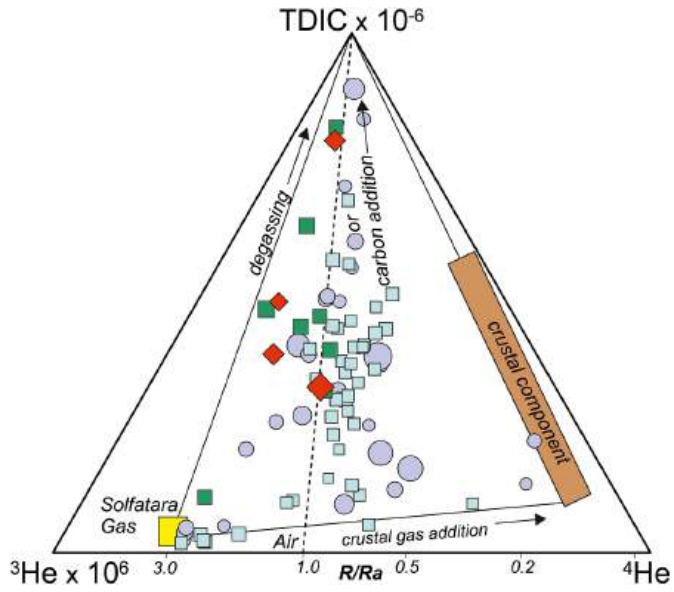

Fig. 12. ^{3}He-^{4}He-TDIC triangular plot showing the compositional diversity of dissolved gases in the CFc groundwater. The compositions of possible gas sources involved in mixing processes are also indicated.

multi-step process, starting with (i) the initial infiltration of air-saturated groundwater, followed by (ii) pressurization by dissolution (ingassing) of a CO_2-He-rich magmatic-hydrothermal vapor during downward water inflow in the caldera central segment, eventually with some addition of crustal gases (for both CO_2 and He), and finally (iii) degassing of more water-insoluble species (He, N_2, Ar, CH_4) during groundwater upflow and decompression to 1 bar.

We model this sequence of processes by applying a gas-water-rock reaction-path model that numerically simulates the interaction among water, gas and rock within the shallow volcanic aquifers. The model simulates the evolution of the chemical and carbon isotopic composition of groundwater affected by the input of a hydrothermal Solfatara-like CO_2-rich gas phase. The simulation has been done by use of the PHREEQC code (Parkhurst and Appelo, 1999), associated with a VBA (Visual Basic for Application) script to write the input file, run the executable code, read and elaborate the output files, and compute the carbon isotopic composition of each carbon species (in solution and degassed) at each step of the model. The PHREEQC database has been integrated with thermodynamic data of the investigated gas species (N_2, O_2, Ar, Ne, He) taken from Wilhelm et al. (1977) and considered as non-reactive species in the models. Rigorous simulation of water-rock interaction would require considering dissolution of primary minerals and formation of alteration minerals. However, for simplicity, we approach the simulation not relying on a purely thermodynamic approach, but rather based on empirical functions established from the chemical composition of the investigated groundwater (Fig. 13). In particular, to quantify the interaction between water, rocks and hydrothermal gas during the reaction pathway modelling, we utilize the relationship between carbonate bound cations (CBC) and the corresponding TDIC value (Fig. 13). CBC quantifies the extent of dissolution of primary volcanic minerals, and is computed by subtracting the sum of chloride, nitrate and sulphate equivalents from the sum of Ca, Mg, Na and K. In other words, CBC corresponds to alkalinity in charge-balanced analysis. TDIC is computed at discharged condition for the samples undersaturated with respect to calcite and, for the samples oversaturated with respect to calcite, TDIC is computed by bringing the solutions back to equilibrium conditions with respect to calcite by adding CO_2 (see Caliro et al., 2005).

The model simulates the composition of major ions, dissolved gases, and their isotopic compositions at depth (RC, reservoirs conditions) and at the surface (ES, emergence conditions). Deep conditions are simulated assuming that no chemical and isotopic fractionation occurs during addition of gases to the solution (for more details see Wigley et al., 1978, 1979). Degassing does not take place at this stage because of the relatively high hydrostatic pressures. While approaching emergence/spring conditions, the solution is allowed to degas in chemical and isotopic equilibrium at decreasing pressures in a multistep process from condition reached at depth to a gas pressure of 1 bar at the surface. For the samples that are supersaturated at emergence conditions, the minimum pressure at reservoir conditions can be estimated by bringing the sample back into equilibrium with respect to the calcite.

Table 2
The average composition of Solfatara BG fumarole in 2013. Concentrations are in μmol/mol. Carbon isotopic composition is expressed in delta notation per mill vs. V-PDB;

CO_2(g)	2.57E+05
Ar(g)	6.36E-01
N_2(g)	4.99E+02
He(g)	2.47E+00
Ne(g)	8.22E-03
$\delta^{13}C$	-1.3‰

The CFc solution carbonate system shows that the samples exhibiting low TDIC concentrations have negative $\delta^{13}C$ values ($\delta^{13}C < \sim -10$ ‰), while samples with higher TDIC have the most positive $\delta^{13}C$ values (Fig. 8). This behavior implies the presence of different carbon sources. Carbon-13-depleted composition suggests a biologic origin, while more positive $\delta^{13}C$ values (^{13}C enriched) might indicate a deep magmatic/hydrothermal source, similar to the fumarolic fluids emitted at Solfatara ($\delta^{13}C$ -1.3 ‰ Caliro et al., 2007).

We start the models by equilibrating a meteoric water with a TDIC of ~1 mmol/L and $\delta^{13}C$ of −8 ‰ at 1 bar and 20 °C with atmospheric components (N_2, O_2, Ar, He). CO_2 with biologic isotopic composition from $\delta^{13}C$ -25 ‰ to −15 ‰ is systematically added to this solution (Fig. 8). Most of the bicarbonate cold waters (Fig. 8) are in agreement

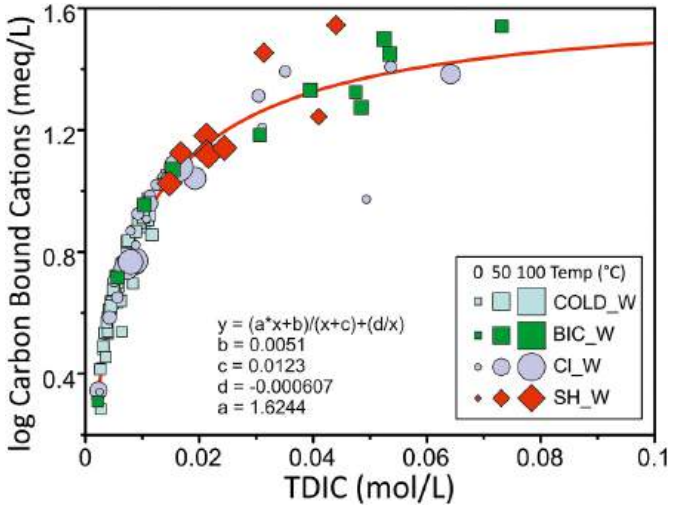

Fig. 13. Log concentrations of Carbon Bound Cations (∑(Ca, Mg, Na, K)- ∑(Cl, NO_3, SO_4) in meq/L) vs. TDIC. The relation (red line) was used in the reaction-path modelling to compute the amount of carbonate bound cations dissolved by the addition of the deep gas phase. (For interpretation of the references to colour in this figure legend, the reader is referred to the web version of this article.)

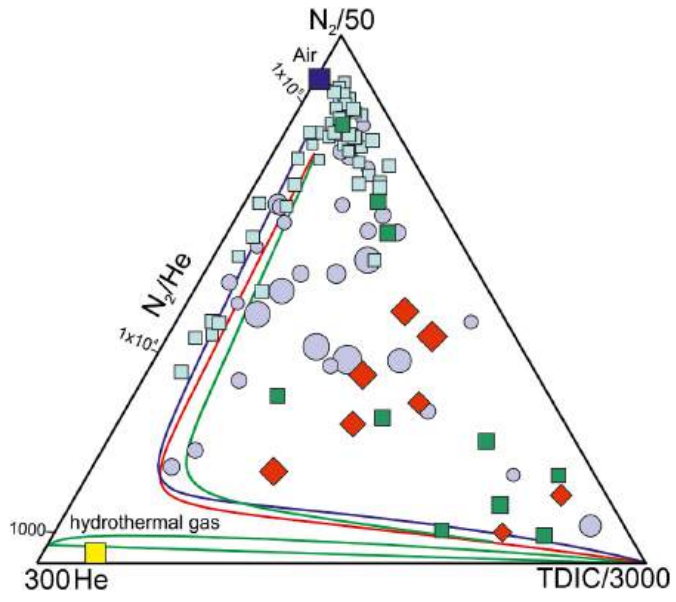

Fig. 14. Dissolved gas species N_2, He and TDIC in CFc groundwater showing compositional evolution lines resulting from the models. The models start from the N_2-rich air/asw composition. Hydrothermal gas input moves compositions towards a He-rich composition until degassing becomes predominant, resulting in loss of He and enrichment of carbon species. Light green lines indicate the composition of the degassed gas phase. (For interpretation of the references to colour in this figure legend, the reader is referred to the web version of this article.)

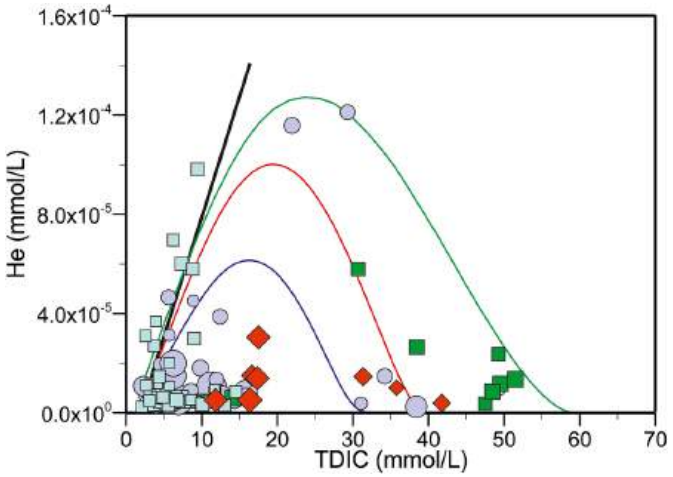

Fig. 15. He vs. TDIC concentrations in the CFc groundwater. Conditions modeled in the reservoir (black line) and the lines resulting after degassing to atmospheric pressure are also reported. The addition of gases to the solution, and the consequent increase of solution temperature, increase the gas-pressure, inducing degassing and in particular He loss, as shown by the BIC_W and SH_W groundwaters, respectively.

with these models, indicating input of biologic carbon, while the other water types require a distinct carbon source. Using as starting solutions the compositions at 2 and 3 mmol/L of TDIC obtained in the previous model (−25 ‰), three simulations were done at different temperatures (25–60-80 °C; Fig. 8) adding to the solutions a hydrothermal Solfatara-like gas phase with composition reported in Table 2. 0.1 mol of this gas phase are added to the solution in 100 steps, adding CBC to the solution following the relation of Fig. 13. At each step, after dissolution of the gas phase, the solution is allowed to degas to atmospheric pressure. The model lines reported in Figs. 8, 14 and 15 refer to the solutions after degassing at discharge conditions (PHREEQC files for the 60 °C model are in the Supplementary Material S2 and S3).

Most of the water samples are in good agreement with the proposed models, showing that a combination of (i) input of a Solfatara-like hydrothermal gas phase and (ii) degassing from reservoir conditions to the shallow conditions can account for the dissolved gas and dissolved carbon isotopic compositions. Data variability of samples plotting out of the modelling lines can be explained by the mixing process, as discussed in the previous sections.

7. Conclusions and implications for volcano monitoring

We have shown here that the large diversity in groundwater composition at CFc reflects the combined action of a variety of processes, including (i) infiltration of shallow meteoric/marine waters in the aquifer(s), (ii) their chemical processing and maturation, initiated by the dissolution of deeply sourced magmatic volatiles, and modulated by the mixing with hydrothermal brines ascending from deeper hydrothermal reservoirs, and (iii) further chemical evolution during upward groundwater flow (to the emission/sampling point), primarily driven by degassing of poorly soluble gases (N_2, Ar, He, CH_4) and condensation of hot hydrothermal steam (primarily in the Solfatara-Pisciarelli sector). These processes act in concert, but their relative roles vary in space determining the chemical heterogeneity of the aquifer system, as summarized in the cross-section of Fig. 16. This Figure also illustrates the estimated temperature and fluids circulation patterns resulting from the 3D physical modelling of the CFc hydrothermal system (Petrillo et al., 2013). This scheme also emphasizes the role of volcano-tectonic structures (taken from a WSW-ENE section of Orsi et al., 1996) in controlling the migration of fluids (CO_2 gas and aqueous solutions), as inferred from the physical model of CFc hydrothermal system (Petrillo et al., 2013).

The processes depicted in Fig. 16 may also vary in time if the ongoing unrest escalates further. This aspect is especially valuable in terms of volcano monitoring because, as seen elsewhere (see review in Jasim et al., 2018), any change in groundwater composition would ultimately respond to changes in hydrothermal regime, and hence in caldera activity state.

The Solfatara-Pisciarelli district has recently experienced remarkable changes in hydrothermal activity, with notable variations in fumarole composition (Chiodini et al., 2016, 2021, 2022; Caliro et al., 2025) and increases in the CO_2 output from soil diffuse degassing (Cardellini et al., 2017) and fumaroles (Aiuppa et al., 2013; Tamburello et al., 2019). Taken together, these observations imply an escalating transport of magma-sourced volatiles to the Solfatara-Pisciarelli hydrothermal system (Chiodini et al., 2022), causing pressure build-up at depth (Chiodini et al., 2021) and hence rock failure (the Solfatara-Pisciarelli zone and its surroundings are the areas where the majority of the CFc seismicity is

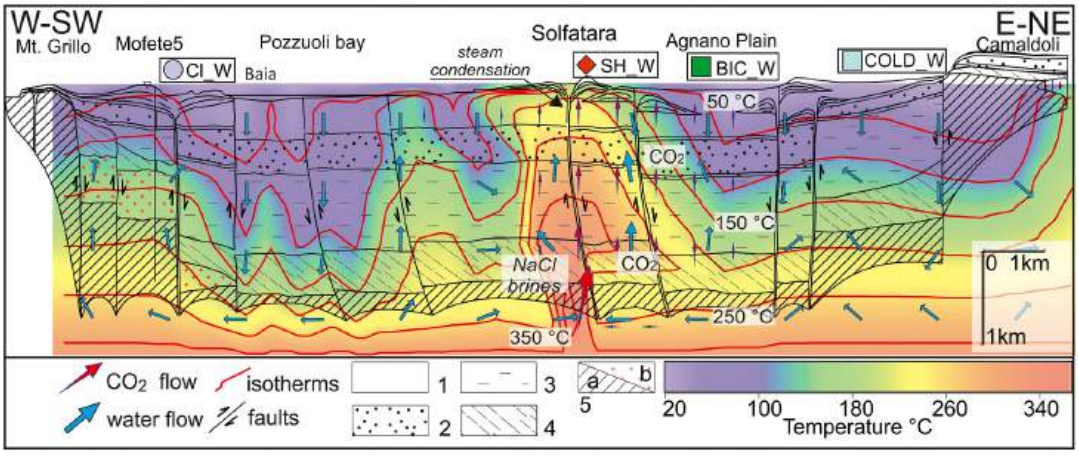

Fig. 16. Conceptual model for the diversity of CF groundwaters in the context of the results of the 3D physical model of the Campi Flegrei geothermal system (Petrillo et al., 2013). The geological section of the CF caldera, shown as background, is from Orsi et al. (1996). The main processes concurring to the definition of chemical and isotopic composition of groundwater and thermal water are also indicated The predominant effect on the fluids circulation is represented by a central plume below the Solfatara crater that activate convective cells, producing variable patterns of gas, liquid and temperature inside the hydrothermal system. Geological section (modified after Orsi et al., 1996): (1) Volcanics and marine sediments younger than 15 ka; (2) Neapolitan Yellow Tuff (NYT); (3) Volcanics and marine sediments emplaced between 39 and 15 ka; (4) Campanian Ignimbrite (CI); 5 Rocks older than 39 ka, a) pyroclastics, b) lavas. (For interpretation of the references to colour in this figure legend, the reader is referred to the web version of this article.)

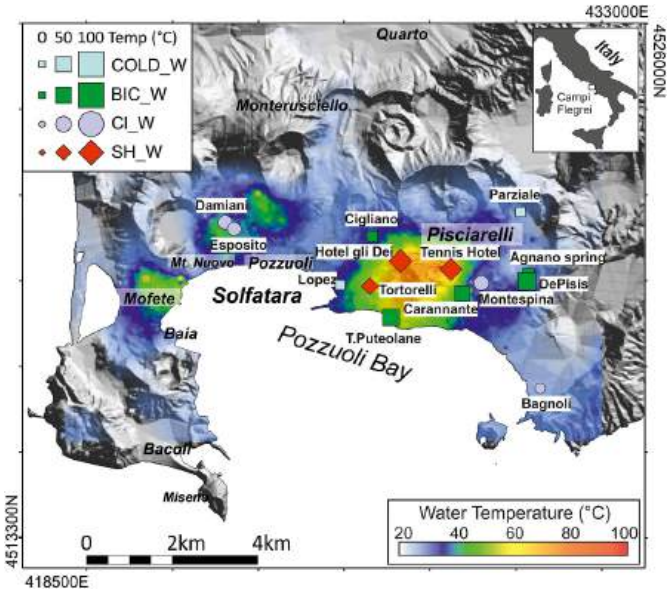

Fig. 17. Multi-parameter groundwater monitoring network (temperature, salinity and piezometric level) consisting of 14 stations covering a wide area surrounding Solfatara, active since 2018. Symbols as in Fig. 2.

clustered; Scarpa et al., 2022; Giacomuzzi et al., 2024).

In response to the increase in volcanic activity and in order to improve the monitoring network system within the agreement for the Seismic and Volcanic Surveillance between the Italian Department of Civil Protection and the INGV (National Institute of Geophysics and Volcanology), since 2018 a permanent network of stations for continuous multi-parametric monitoring of the CF groundwater has been developed and implemented at CFc (Fig. 17). The installed CTD systems have shown excellent sensitivity and stability over time, allowing to identify seasonal variations, linked to meteorological events. Moreover, data recorded by this network allowed to recognize rapid changes in water temperature, water level and salinity in response to phases of especially intense seismicity activity and accelerating ground deformation, which are the subject of ongoing investigation (and will be presented elsewhere).

We have shown here that groundwater chemistry in the Solfatara-Pisciarelli district is primarily controlled by near-surface condensation of the hydrothermal steam plume feeding the Solfatara fumaroles. We argue then that continuous measurement of groundwater temperature, piezometric level and conductivity in this area may reveal critical to identifying any further escalation in hydrothermal steam transport, would the degassing unrest intensifies further. In more marginal areas relative to center of deformation (Pozzuoli city) and degassing (Solfatara-Pisciarelli), such as in the Agnano plain and in the Baia-Monte Nuovo sectors (Fig. 1), the chemistry of thermal groundwater primarily reflects the addition of deeply sourced CO_2 (BIC_W) and mixing with deeply rising (Mofete reservoir-like) hydrothermal brines (Cl_W). In these sectors, permanent groundwater monitoring (Fig. 17) may help identifying any stress change and/or change in fluid circulation pathways, and especially if the mixing proportions between different water types, or the supply of deeply sources gases/brines, vary in time in response to changes in the hydrothermal-magmatic system underneath. Visible variations in well water outflow and temperature have been documented in historical records prior to the last CFc eruption in 1538 AD (Guidoboni and Ciuccarelli, 2011), which adds confidence on the ability of a modern instrumental network (as the one implemented at CFc; Fig. 17) to detect any further change in hydrothermal regime.

CRediT authorship contribution statement

Stefano Caliro: Writing – review & editing, Writing – original draft, Methodology, Investigation, Funding acquisition, Formal analysis, Data curation, Conceptualization, Supervision. **Rosario Avino:** Writing – review & editing, Investigation, Formal analysis, Data curation. **Francesco Capecchiacci:** Writing – review & editing, Writing – original draft, Methodology, Investigation, Formal analysis, Data curation. **Antonio Carandente:** Writing – review & editing, Investigation, Formal analysis, Data curation. **Giovanni Chiodini:** Writing – review & editing, Writing – original draft, Validation, Methodology, Formal analysis, Data curation, Conceptualization. **Emilio Cuoco:** Writing – review & editing, Investigation, Formal analysis, Data curation. **Carmine Minopoli:** Writing – review & editing, Writing – original draft, Investigation, Formal analysis, Data curation. **Francesco Rufino:** Writing – review & editing, Investigation, Formal analysis, Data curation. **Alessandro Santi:** Writing – review & editing, Investigation, Formal analysis, Data curation. **Andrea L. Rizzo:** Writing – review & editing, Methodology, Formal analysis, Data curation. **Alessandro Aiuppa:** Writing – review & editing, Writing – original draft, Validation, Methodology, Formal analysis, Conceptualization, Supervision. **Vincenzo Allocca:** Writing – review & editing, Writing – original draft, Methodology, Formal analysis, Data curation. **Pantaleone De Vita:** Writing – review & editing, Writing – original draft, Methodology, Formal analysis, Data curation. **Mauro A. Di Vito:** Writing – review & editing, Writing – original draft, Validation, Investigation, Formal analysis, Data curation, Conceptualization.

Declaration of competing interest

The authors declare the following financial interests/personal relationships which may be considered as potential competing interests:

Stefano Caliro reports financial support was provided by Dipartimento della Protezione Civile, Presidenza del Consiglio dei Ministri. If there are other authors, they declare that they have no known competing financial interests or personal relationships that could have appeared to influence the work reported in this paper.

Acknowledgments

Data were acquired in the framework of the Campi Flegrei volcanic surveillance funded by the Italian Dipartimento della Protezione Civile, Presidenza del Consiglio dei Ministri (DPC) Conv. DPC-INGV 2022-2024 and 2024-2026. This paper does not necessarily represent DPC official opinion and policies. We thank Steven Ingebritsen from California Volcano Observatory and another anonymous reviewer for their constructive comments on the manuscript. We are grateful to Mariano Tantillo from INGV-Palermo for the isotopic analyses of noble gases.

Appendix A. Supplementary data

Supplementary data to this article can be found online at https://doi.org/10.1016/j.jvolgeores.2025.108280.

Data availability

Data used in this work are uploaded as S1 table; input and output file of the proposed model are reportes as S2 and S3 supplementary material, respectively.

References

Aiuppa, A., Avino, R., Brusca, L., Caliro, S., Chiodini, G., D'Alessandro, W., Favara, R., Federico, C., Ginevra, W., Inguaggiato, S., Longo, M., Pecoraino, G., Valenza, M., 2006. Mineral control of arsenic content in thermal waters from volcano-hosted hydrothermal systems: insights from island of Ischia and Phlegrean Fields

(Campanian Volcanic Province, Italy). Chem. Geol. 229 (4), 313–330. https://doi.org/10.1016/j.chemgeo.2005.11.004.
Aiuppa, A., Tamburello, G., Di Napoli, R., Cardellini, C., Chiodini, G., Giudice, G., Grassa, F., Pedone, M., 2013. First observations of the fumarolic gas output from a restless caldera: implications for the current period of unrest (2005-2013) at Campi Flegrei. Geochem. Geophys. Geosyst. 14 (10). https://doi.org/10.1002/ggge.20261.
Allocca, V., Coda, S., De Vita, P., Di Rienzo, B., Ferrara, L., Giarra, A., Mangoni, O., Stellato, L., Trifuoggi, M., Arienzo, M., 2018. Hydrogeological and hydrogeochemical study of a volcanic-sedimentary coastal aquifer in the archaeological site of Cumae (Phlegraean Fields, southern Italy). J. Geochem. Explor. 185, 105–115. https://doi.org/10.1016/j.gexplo.2017.11.004.
Baldi, P., Ferrara, G.C., Panichi, C., 1975. Geothermal research in western Campania (southern Italy): chemical and isotopic studies of thermal fluids in the Campi Flegrei. In: Proceedings of the 2nd U.N. Symp. on Development and Use of Geothermal Resources, San Francisco, pp. 687–697.
Ballentine, C.J., Burgess, R., Marty, B., 2002. Tracing Fluid Origin, Transport and Interaction in the Crust. In: Porcelli, P.D., Ballentine, C.J., Wieler, R. (Eds.), Noble Gases. De Gruyter, Berlin, Boston, pp. 539–614. https://doi.org/10.1515/9781501509056-015.
Barberi, F., Corrado, G., Innocenti, F., Luongo, G., 1984. Phlegraean Fields 1982–1984: brief chronicle of a volcano emergency in a densely populated area. Bull. Volcanol. 47, 175–185.
Bevilacqua, A., De Martino, P., Giudicepietro, F., Ricciolino, P., Patra, A., Pitman, E.B., Bursik, M., Voight, B., Flandoli, F., Macedonio, G., Neri, A., 2022. Data analysis of the unsteadily accelerating GPS and seismic records at Campi Flegrei caldera from 2000 to 2020. Sci. Rep. 12 (1), 19175. https://doi.org/10.1038/s41598-022-23628-5.
Blockley, S.P.E., Bronk Ramsey, C., Pyle, D.M., 2008. Improved age modelling and high-precision age estimates of late Quaternary tephras, for accurate palaeoclimate reconstruction. J. Volcanol. Geotherm. Res. 177 (1), 251–262. https://doi.org/10.1016/j.jvolgeores.2007.10.015.
Bolognesi, L., Noto, P., Nuti, S., 1986. Studio chimico ed isotopico della solfatara di Pozzuoli: ipotesi sull'origine e sulle temperature profonde dei fluidi. Rend. Soc. It. Mineral. Petrol. 41 (2), 281–295.
Bonfanti, P., D'Alessandro, W., Dongarrà, G., Parello, F., Valenza, M., 1996a. Mt. Etna eruption 1991-93: geochemical anomalies in groundwaters. Acta Vulcanol. 8 (1), 107–109.
Bonfanti, P., DAlessandro, W., Dongarra, G., Parello, F., Valenza, M., 1996b. Medium-term anomalies in groundwater temperature before 1991-1993 Mt Etna eruption. J. Volcanol. Geotherm. Res. 73 (3-4), 303–308. https://doi.org/10.1016/0377-0273(96)00026-1.
Brombach, T., Marini, L., Hunziker, J.C., 2000. Geochemistry of the thermal springs and fumaroles of Basse-Terre Island, Guadeloupe. Lesser Antilles. B Volcanol 61 (7), 477–490. https://doi.org/10.1007/Pl00008913.
Bruno, P.P.G., Ricciardi, G.P., Petrillo, Z., Di Fiore, V., Troiano, A., Chiodini, G., 2007. Geophysical and hydrogeological experiments from a shallow hydrothermal system at Solfatara Volcano, Campi Flegrei, Italy: Response to caldera unrest. J. Geophys. Res. 112 (B6), B06201. https://doi.org/10.1029/2006JB004383.
Buono, G., Caliro, S., Paonita, A., Pappalardo, L., Chiodini, G., 2023. Discriminating carbon dioxide sources during volcanic unrest: The case of Campi Flegrei caldera (Italy). Geology 51 (4), 397–401. https://doi.org/10.1130/g50624.1.
Byrdina, S., Vandemeulebrouck, J., Cardellini, C., Legaz, A., Camerlynck, C., Chiodini, G., Lebourg, T., Gresse, M., Bascou, P., Motos, G., Carrier, A., Caliro, S., 2014. Relations between electrical resistivity, carbon dioxide flux, and self-potential in the shallow hydrothermal system of Solfatara (Phlegrean Fields, Italy). J. Volcanol. Geotherm. Res. 283, 172–182. https://doi.org/10.1016/j.jvolgeores.2014.07.010.
Caliro, S., Panichi, C., Stanzione, D., 1998. Baseline study of the isotopic and chemical composition of waters associated with the Somma Vesuvio volcanic system. Acta Vulcanol. 10, 19–26.
Caliro, S., Panichi, C., Stanzione, D., 1999. Variation in the total dissolved carbon isotope composition of thermal waters of the Island of Ischia (Italy) and its implications for volcanic surveillance. J. Volcanol. Geotherm. Res. 90 (3-4), 219–240. https://doi.org/10.1016/s0377-0273(99)00027-x.
Caliro, S., Caracausi, A., Chiodini, G., Ditta, M., Italiano, F., Longo, M., Minopoli, C., Nuccio, P.M., Paonita, A., Rizzo, A., 2004. Evidence of a recent input of magmatic gases into the quiescent volcanic edifice of Panarea, Aeolian Islands, Italy. Geophys. Res. Lett. 31 (7). https://doi.org/10.1029/2003gl019359.
Caliro, S., Chiodini, G., Avino, R., Cardellini, C., Frondini, F., 2005. Volcanic degassing at Somma-Vesuvio (Italy) inferred by chemical and isotopic signatures of groundwater. Appl. Geochem. 20 (6), 1060–1076. https://doi.org/10.1016/j.apgeochem.2005.02.002.
Caliro, S., Chiodini, G., Moretti, R., Avino, R., Granieri, D., Russo, M., Fiebig, J., 2007. The origin of the fumaroles of La Solfatara (Campi Flegrei, South Italy). Geochim. Cosmochim. Acta 71 (12), 3040–3055. https://doi.org/10.1016/j.gca.2007.04.007.
Caliro, S., Chiodini, G., Izzo, G., Minopoli, C., Signorini, A., Avino, R., Granieri, D., 2008. Geochemical and biochemical evidence of lake overturn and fish kill at Lake Averno, Italy. J. Volcanol. Geotherm. Res. 178 (2), 305–316. https://doi.org/10.1016/j.jvolgeores.2008.06.023.
Caliro, S., Chiodini, G., Paonita, A., 2014. Geochemical evidences of magma dynamics at Campi Flegrei (Italy). Geochim. Cosmochim. Acta 132 (1), 1–15. https://doi.org/10.1016/j.gca.2014.01.021.
Caliro, S., Chiodini, G., Avino, R., Carandente, A., Cuoco, E., Di Vito, M.A., Minopoli, C., Rufino, F., Santi, A., Lages, J., Mangiacapra, A., Monteleone, B., Pappalardo, L., Taracsák, Z., Tramati, C., Vizzini, S., Aiuppa, A., 2025. Escalation of caldera unrest indicated by increasing emission of isotopically light sulfur. Nat. Geosci. https://doi.org/10.1038/s41561-024-01632-w (*in press*).
Capasso, G., Favara, R., Francofonte, S., Inguaggiato, S., 1999. Chemical and isotopic variations in fumarolic discharge and thermal waters at Vulcano Island (Aeolian Islands, Italy) during 1996: evidence of resumed volcanic activity. J. Volcanol. Geotherm. Res. 88 (3), 167–175. https://doi.org/10.1016/S0377-0273(98)00111-5.
Caprarelli, G., Tsutsumi, M., Turi, B., 1997. Chemical and isotopic signatures of the basement rocks from the Campi Flegrei geothermal field (Naples, southern Italy): inferences about the origin and evolution of its hydrothermal fluids. J. Volcanol. Geotherm. Res. 76 (1), 63–82. https://doi.org/10.1016/S0377-0273(96)00072-8.
Cardellini, C., Chiodini, G., Frondini, F., Avino, R., Bagnato, E., Caliro, S., Lelli, M., Rosiello, A., 2017. Monitoring diffuse volcanic degassing during volcanic unrests: the case of Campi Flegrei (Italy). Sci. Rep. 7 (1), 6757. https://doi.org/10.1038/s41598-017-06941-2.
Celico, P., De Gennaro, M., Pagano, D., Ronca, A., Stanzione, D., Vallario, A., 1987. Idrogeologia e idrogeochimica dei Campi Flegrei: relazioni tra chimismo delle acque e idrodinamica sotterranea. Atti Convegno" Bradisismo e fenomeni connessi", Napoli 19 (20), 94–100.
Celico, P., De Vita, P., Nikzad, F., Stanzione, D., Vallario, A., 1991. Schema idrogeologico e idrogeochimico dei Campi Flegrei (NA). AttiIConveg. Nazion. Giovani Ricercat. Geol. Appl. Gargnano 287–296.
Celico, P., Dall'Aglio, M., Ghiara, M.R., Stanzione, D., Brondi, M., Prosperi, M., 1992. Geochemical monitoring of the thermal fluids in the Phlegraean Fields from 1970 to 1990. Ital. J. Geosci. 111 (3-4), 409–422.
Chiodini, G., Cioni, R., Marini, L., Panichi, C., 1996. Origin of the fumarolic fluids of Vulcano Island, Italy and implications for volcanic surveillance - Reply. B Volcanol. 58 (4), 321–322.
Chiodini, G., Frondini, F., Cardellini, C., Granieri, D., Marini, L., Ventura, G., 2001. CO_2 degassing and energy release at Solfatara volcano, Campi Flegrei, Italy. J. Geophys. Res. 106 (B8), 16213–16221. https://doi.org/10.1029/2001jb000246.
Chiodini, G., Todesco, M., Caliro, S., Del Gaudio, C., Macedonio, G., Russo, M., 2003. Magma degassing as a trigger of bradyseismic events; the case of Phlegrean Fields (Italy). Geophys. Res. Lett. 30 (8), 1434. https://doi.org/10.1029/2002GL016790.
Chiodini, G., Caliro, S., De Martino, P., Avino, R., Gherardi, F., 2012. Early signals of new volcanic unrest at Campi Flegrei caldera? Insights from geochemical data and physical simulations. Geology 40 (10), 943–946. https://doi.org/10.1130/g33251.1.
Chiodini, G., Pappalardo, L., Aiuppa, A., Caliro, S., 2015. The geological CO2 degassing history of a long-lived caldera. Geology 43 (9), 767–770. https://doi.org/10.1130/G36905.1.
Chiodini, G., Paonita, A., Aiuppa, A., Costa, A., Caliro, S., De Martino, P., Acocella, V., Vandemeulebrouck, J., 2016. Magmas near the critical degassing pressure drive volcanic unrest towards a critical state. Nat. Commun. 7, 13712. https://doi.org/10.1038/ncomms13712.
Chiodini, G., Caliro, S., Avino, R., Bini, G., Giudicepietro, F., De Cesare, W., Ricciolino, P., Aiuppa, A., Cardellini, C., Petrillo, Z., Selva, J., Siniscalchi, A., Tripaldi, S., 2021. Hydrothermal pressure-temperature control on CO2 emissions and seismicity at Campi Flegrei (Italy). J. Volcanol. Geotherm. Res. 414. https://doi.org/10.1016/j.jvolgeores.2021.107245.
Chiodini, G., 1996. Gases dissolved in groundwaters: analyticalmethods and examples of applications in central Italy. In: Marini, L., Ottonello, G. (Eds.), Rome Seminar on Environmental Geochemistry. Pacini Editore, Castelnuovo, di Porto, Rome (Italy), pp. 135–148.
Chiodini, G., Caliro, S., Avino, R., Bagnato, E., Capecchiacci, F., Carandente, A., Cardellini, C., Minopoli, C., Tamburello, G., Tripaldi, S., 2022. The Hydrothermal System of the Campi Flegrei Caldera, Italy, Campi Flegrei: A Restless Caldera in a Densely Populated Area. Springer, Berlin Heidelberg Berlin, Heidelberg, pp. 239–255.
Cioni, R., Corazza, E., Marini, L., 1984. The gas/steam ratio as indicator of heat transfer at the Solfatara fumaroles, Phlegraean Fields (Italy). Bull. Volcanol. 47, 295–302.
Corrado, G., Guerra, I., Lo Bascio, A., Luongo, G., Rampoldi, F., 1977. Inflation and microearthquake activity of Phlegraean Fields. Italy. Bull Volcanol. 40 (3), 169–188. https://doi.org/10.1007/BF02596998.
Cronan, D., Johnson, A., Hodkinson, R., 1997. Hydrothermal fluids may offer clues about impending volcanic eruptions. EOS Trans. Am. Geophys. Union 78 (33), 341–345.
Dall'Aglio, M., Martini, M., Tonani, F., 1972. Rilevamento Geochimico delle Emanazioni Vulcaniche dei Campi Flegrei; Etude Geochimique des Emanations Volcaniques des Champs Phlegreens. Quad. Ric. Sci. Ital. 0083, 152–181.
D'Auria, L., Giudicepietro, F., Aquino, I., Borriello, G., Del Gaudio, C., Lo Bascio, D., Martini, M., Ricciardi, G.P., Ricciolino, P., Ricco, C., 2011. Repeated fluid-transfer episodes as a mechanism for the recent dynamics of Campi Flegrei Caldera (1989-2010). J. Geophys. Res. 116 (B4), B04313. https://doi.org/10.1029/2010JB007837.
D'Auria, L., Pepe, S., Castaldo, R., Giudicepietro, F., Macedonio, G., Ricciolino, P., Tizzani, P., Casu, F., Lanari, R., Manzo, M., Martini, M., Sansosti, E., Zinno, I., 2015. Magma injection beneath the urban area of Naples: a new mechanism for the 2012–2013 volcanic unrest at Campi Flegrei caldera. Sci. Rep. 5, 13100. https://doi.org/10.1038/srep13100.
De Vita, P., Vincenzo, Allocca, Fulvio, Celico, Silvia, Fabbrocino, Cesaria, Mattia, Giuseppina, Monacelli, Ilaria, Musilli, Vincenzo, Piscopo, Rosa, Scalise Anna, Summa, G., Giuseppe, I. Tranfaglia, Celico, P., 2018. Hydrogeology of continental southern Italy. J. Maps 14 (2), 230–241. https://doi.org/10.1080/17445647.2018.1454352.
De Vivo, B., Belkin, H.E., Barbieri, M., Chelini, W., Lattanzi, P., Lima, A., Tolomeo, L., 1989. The Campi Flegrei (Italy) geothermal system: a fluid inclusion study of the Mofete and San Vito fields. J. Volcanol. Geotherm. Res. 36 (4), 303–326.
Del Gaudio, C., Aquino, I., Ricciardi, G.P., Ricco, C., Scandone, R., 2010. Unrest episodes at Campi Flegrei: a reconstruction of vertical ground movements during 1905–2009.

J. Volcanol. Geotherm. Res. 195 (1), 48–56. https://doi.org/10.1016/j.jvolgeores.2010.05.014.
Delmelle, P., Kusakabe, M., Bernard, A., Fischer, T., de Brouwer, S., del Mundo, E., 1998. Geochemical and isotopic evidence for seawater contamination of the hydrothermal system of Taal Volcano, Luzon, the Philippines. Bull. Volcanol. 59 (8), 562–576. https://doi.org/10.1007/s004450050210.
Deutsch, C., Journel, A., 1998. Applied Geostatistics. Oxford University Press, New York.
Di Napoli, R., Aiuppa, A., Sulli, A., Caliro, S., Chiodini, G., Acocella, V., Ciraolo, G., Di Vito, M.A., Interbartolo, F., Nasello, C., Valenza, M., 2016. Hydrothermal fluid venting in the offshore sector of Campi Flegrei caldera: a geochemical, geophysical, and volcanological study. Geochem. Geophys. Geosyst. 17 (10), 4153–4178. https://doi.org/10.1002/2016gc006494.
Di Vito, M.A., Isaia, R., Orsi, G., Southon, J., De Vita, S., D'Antonio, M., Pappalardo, L., Piochi, M., 1999. Volcanism and deformation since 12,000 years at the Campi Flegrei caldera (Italy). J. Volcanol. Geotherm. Res. 91 (2-4), 221–246. https://doi.org/10.1016/S0377-0273(99)00037-2.
Di Vito, M.A., Acocella, V., Aiello, G., Barra, D., Battaglia, M., Carandente, A., Del Gaudio, C., de Vita, S., Ricciardi, G.P., Ricco, C., Scandone, R., Terrasi, F., 2016. Magma transfer at Campi Flegrei caldera (Italy) before the 1538 AD eruption. Sci. Rep. 6 (1), 32245. https://doi.org/10.1038/srep32245.
Evans, W.C., van Soest, M.C., Mariner, R.H., Hurwitz, S., Ingebritsen, S.E., Wicks, C.W., Schmidt, M.E., 2004. Magmatic intrusion west of Three sisters, Central Oregon, USA: the perspective from spring geochemistry. Geology 32 (1), 69–72. https://doi.org/10.1130/G19974.1.
Federico, C., Aiuppa, A., Favara, R., Gurrieri, S., Valenza, M., 2004. Geochemical monitoring of groundwaters (1998-2001) at Vesuvius volcano (Italy). J. Volcanol. Geotherm. Res. 133 (1-4), 81–104. https://doi.org/10.1016/S0377-0273(03)00392-5.
Federico, C., Cocina, O., Gambino, S., Paonita, A., Branca, S., Coltelli, M., Italiano, F., Bruno, V., Caltabiano, T., Camarda, M., Capasso, G., De Gregorio, S., Diliberto, I.S., Di Martino, R.M.R., Falsaperla, S., Greco, F., Pecoraino, G., Salerno, G., Sciotto, M., Bellomo, S., Grazia, G.D., Ferrari, F., Gattuso, A., La Pica, L., Mattia, M., Pisciotta, A. F., Pruiti, L., Sortino, F., 2023. Inferences on the 2021 ongoing volcanic unrest at Vulcano Island (Italy) through a comprehensive multidisciplinary surveillance network. Remote Sens-Basel. 15 (5). https://doi.org/10.3390/rs15051405.
Ghiara, M.R., Stanzione, D., 1988. Studio geochimico sul sistema idrotermale dei Campi Flegrei (Campania, Italia). Rendicon. dell'Accad. delle Sci. Fisiche Matemat. 55, 61–83.
Giacomuzzi, G., Chiarabba, C., Bianco, F., De Gori, P., Agostinetti, N.P., 2024. Tracking transient changes in the plumbing system at Campi Flegrei Caldera. Earth Planet. Sci. Lett. 637, 118744. https://doi.org/10.1016/j.epsl.2024.118744.
Giggenbach, W.F., 1988. Geothermal solute equilibria. Derivation of Na-K-Mg-Ca geoindicators. Geochim. Cosmochim. Acta 52 (12), 2749. https://doi.org/10.1016/0016-7037(88)90143-3.
Giggenbach, W.F., Stewart, M.K., 1982. Processes controlling the isotopic composition of steam and water discharges from steam vents and steam-heated pools in geothermal areas. Geothermics 11 (2), 71. https://doi.org/10.1016/0375-6505(82)90009-8.
Giggenbach, W.F., Gonfiantini, R., Jangi, B.L., Truesdell, A.H., 1983. Isotopic and chemical composition of Parbati Valley geothermal discharges, North-West Himalaya, India. Geothermics 12 (2-3), 199.
Goff, F., Janik, C.J., 2000. Geothermal Systems. In: Sigurdsson, H., Houghton, B., McNutt, S., Rymer, H., Stix, J. (Eds.), Encyclopedia of Volcanoes. Academic Press, San Diego, CA, pp. 817–834.
Goff, F., McMurtry, G.M., Counce, D., Simac, J.A., Roldán-Manzo, A.R., Hilton, D.R., 2000. Contrasting hydrothermal activity at Sierra Negra and Alcedo volcanoes, Galapagos Archipelago, Ecuador. B Volcanol 62 (1), 34–52. https://doi.org/10.1007/s004450050289.
Graham, D.W., 2002. Noble gas isotope geochemistry of mid-ocean and ocean island basalts: characterization of mantle source reservoirs. Rev. Mineral. Geochem. 47, 247–317. https://doi.org/10.2138/rmg.2002.47.8.
Gresse, M., Vandemeulebrouck, J., Byrdina, S., Chiodini, G., Revil, A., Johnson, T.C., Ricci, T., Vilardo, G., Mangiacapra, A., Lebourg, T., Grangeon, J., Bascou, P., Metral, L., 2017. Three-dimensional electrical resistivity tomography of the Solfatara Crater (Italy): implication for the multiphase flow structure of the shallow hydrothermal system. J. Geophys. Res.-Sol. Ea 122 (11), 8749–8768. https://doi.org/10.1002/2017jb014389.
Guglielminetti, M., 1986. Mofete geothermal field. Geothermics 15 (5), 781–790. https://doi.org/10.1016/0375-6505(86)90091-X.
Guidoboni, E., Ciuccarelli, C., 2011. The Campi Flegrei caldera: historical revision and new data on seismic crises, bradyseisms, the Monte Nuovo eruption and ensuing earthquakes (twelfth century 1582 ad). B Volcanol. 73 (6), 655–677. https://doi.org/10.1007/s00445-010-0430-3.
Hemmings, B., Whitaker, F., Gottsmann, J., Hughes, A., 2015. Hydrogeology of Montserrat, review and new insights. J Hydrol: Reg Stud 3, 1–30.
Horita, J., Wesolowski, D.J., 1994. Liquid-vapor fractionation of oxygen and hydrogen isotopes of water from the freezing to the critical temperature. Geochim. Cosmochim. Acta 58 (16), 3425–3437. https://doi.org/10.1016/0016-7037(94)90096-5.
Inguaggiato, S., Rizzo, A., 2004. Dissolved helium isotope ratios in ground-waters: a new technique based on gas-water re-equilibration and its application to Stromboli volcanic system. Appl. Geochem. 19 (5), 665–673. https://doi.org/10.1016/j.apgeochem.2003.10.009.
Isaia, R., Vitale, S., Di Giuseppe, M.G., Iannuzzi, E., D'Assisi Tramparulo, F., Troiano, A., 2015. Stratigraphy, structure, and volcano-tectonic evolution of Solfatara maar-diatreme (Campi Flegrei, Italy). GSA Bull. 127 (9-10), 1485–1504. https://doi.org/10.1130/b31183.1.
Isaia, R., Di Giuseppe, M.G., Natale, J., Tramparulo, F.D.A., Troiano, A., Vitale, S., 2021. Volcano-tectonic setting of the pisciarelli fumarole field, Campi Flegrei Caldera, Southern Italy: insights into fluid circulation patterns and hazard scenarios. Tectonics 40 (5), e2020TC006227. https://doi.org/10.1029/2020TC006227.
Jasim, A., 2016. Exploring the complexity of groundwater flow in volcanic terrains: a combined numerical, experimental and field data approach. Ph.D. thesis, 199. University of Bristol, UK.
Jasim, A., Whitaker, F.F., AC, R, 2015. Impact of channelized flow on temperature distribution and fluid flow in restless calderas: insight from Campi Flegrei caldera, Italy. J. Volcanol. Geoth. Res. 303, 157–174.
Jasim, A., Hemmings, B., Mayer, K., Scheu, B., 2018. Groundwater flow and volcanic unrest, volcanic unrest. Adv. Volcanol. 83–99. https://doi.org/10.1007/11157_2018_33.
Kilburn, C., De Natale, G., Carlino, S., 2017. Progressive approach to eruption at Campi Flegrei caldera in southern Italy. Nat. Commun. 8, 15312. https://doi.org/10.1038/ncomms15312.
Kilburn, C.R.J., Carlino, S., Danesi, S., Pino, N.A., 2023. Potential for rupture before eruption at Campi Flegrei caldera, Southern Italy. Commun. Earth Environ. 4 (1), 190. https://doi.org/10.1038/s43247-023-00842-1.
Lewicki, J.L., Fischer, T., Williams, S.N., 2000. Chemical and isotopic compositions of fluids at Cumbal Volcano, Colombia: evidence for magmatic contribution. B Volcanol. 62 (4-5), 347–361. https://doi.org/10.1007/s004450000100.
Lowenstern, J.B., Hurwitz, S., 2008. Monitoring a supervolcano in repose: heat and volatile flux at the yellowstone caldera. Elements 4 (1), 35–40. https://doi.org/10.2113/Gselements.4.1.35.
Marini, L., Principe, C., Lelli, M., 2022. The Solfatara Magmatic-Hydrothermal System. Springer.
Martelli, M., Nuccio, P.M., Stuart, F.M., Burgess, R., Ellam, R.M., Italiano, F., 2004. Helium-strontium isotope constraints on mantle evolution beneath the Roman Comagmatic Province, Italy. Earth Planet. Sci. Lett. 224 (3-4), 295–308. https://doi.org/10.1016/j.epsl.2004.05.025.
Martini, 1986. Thermal activity and ground deformation at Phlegrean Fields, Italy: precursors of eruptions or fluctuations of quiescent volcanism? A contribution of geochemical studies. JGR Solid Heart 91, 12255–12260. https://doi.org/10.1029/JB091iB12p12255.
Martini, M., Giannini, L., Buccianti, A., Prati, F., Legittimo, P.C., Iozzelli, P., Capaccioni, B., 1991. 1980-1990 - 10 years of geochemical investigation at Phlegrean fields (Italy). J. Volcanol. Geotherm. Res. 48 (1-2), 161–171. https://doi.org/10.1016/0377-0273(91)90040-7.
McCleskey, R.B., Lowenstern, J.B., Schaper, J., Nordstrom, D.K., Heasler, H.P., Mahony, D., 2016. Geothermal solute flux monitoring and the source and fate of solutes in the Snake River, Yellowstone National Park, WY. Appl. Geochem. 73, 142–156. https://doi.org/10.1016/j.apgeochem.2016.08.006.
Orsi, G., D'Antonio, M., Vita, S.D., Gallo, G., 1992. The Neapolitan Yellow Tuff, a large-magnitude trachytic phreatoplinian eruption: eruptive dynamics, magma withdrawal and caldera collapse. J. Volcanol. Geotherm. Res. 53 (1-4). https://doi.org/10.1016/0377-0273(92)90086-S.
Orsi, G., de Vita, S., Di Vito, M., 1996. The restless, resurgent Campi Flegrei nested caldera (Italy): Constraints on its evolution and configuration. J. Volcanol. Geotherm. Res. 74 (3-4), 179–214. https://doi.org/10.1016/S0377-0273(96)00063-7.
Orsi, G., Civetta, L., Del Gaudio, C., de Vita, S., Di Vito, M.A., Isaia, R., Petrazzuoli, S.M., Ricciardi, G.P., Ricco, C., 1999. Short-term ground deformations and seismicity in the resurgent Campi Flegrei caldera (Italy): an example of active block-resurgence in a densely populated area. J. Volcanol. Geotherm. Res. 91 (2), 415–451. https://doi.org/10.1016/S0377-0273(99)00050-5.
Orsi, G., D'Antonio, M., Civetta, L., 2022. Campi Flegrei, A Restless Caldera in a Densely Populated Area. Springer-Verlag GmbH, Germany. https://doi.org/10.1007/978-3-642-37060-1.
Ozima, M., Podosek, F.A., 2002. Noble Gas Geochemistry. Cambridge University Press, UK.
Parkhurst, D.L., Appelo, C., 1999. User's Guide to PHREEQC (Version 2): A Computer Program for Speciation, Batch-reaction, One-Dimensional Transport, and Inverse Geochemical Calculations. US Geological Survey.
Petrillo, Z., Chiodini, G., Mangiacapra, A., Caliro, S., Capuano, P., Russo, G., Cardellini, C., Avino, R., 2013. Defining a 3D physical model for the hydrothermal circulation at Campi Flegrei caldera (Italy). J. Volcanol. Geotherm. Res. 264, 172–182. https://doi.org/10.1016/j.jvolgeores.2013.08.008.
Piper, A.M., 1944. A graphic procedure in the geochemical interpretation of water-analyses. EOS Trans. Am. Geophys. Union 25 (6), 914–928. https://doi.org/10.1029/TR025i006p00914.
Rizzo, A., Grassa, F., Inguaggiato, S., Liotta, M., Longo, M., Madonia, P., Brusca, L., Capasso, G., Morici, S., Rouwet, D., Vita, F., 2009. Geochemical evaluation of observed changes in volcanic activity during the 2007 eruption at Stromboli (Italy). J. Volcanol. Geotherm. Res. 182 (3), 246–254. https://doi.org/10.1016/j.jvolgeores.2008.08.004.
Rizzo, A.L., Federico, C., Inguaggiato, S., Sollami, A., Tantillo, M., Vita, F., et al., 2015. The 2014 effusive eruption at Stromboli volcano (Italy): Inferences from soil CO2 flux and $^{3}He/^{4}He$ ratio in thermal waters. Geophys. Res. Lett. 42 (7), 2235–2243. https://doi.org/10.1002/2014GL062955.
Rolandi, G., Stanzione, D., 1993. Aspetti idrogeologici e idrogeochimici nei Campi Flegrei settentrionali nell'area compresa tra i vulcani Astroni e Pisani. Rend. Accad. Sci. Fis. Mat., Napoli. Ser. IV 60, 215–251.
Rosi, M., Sbrana, A., 1987. Phlegraean Fields. CNR Quaderni de "La Ricerca Scientifica", 9 (114), 175. Rome, Italy.

Sano, Y., Fischer, T.P., 2013. The analysis and interpretation of noble gases in modern hydrothermal systems. In: Burnard, P. (Ed.), The Noble Gases as Geochemical Tracers. Springer, Berlin Heidelberg, Berlin, Heidelberg, pp. 249–317. https://doi.org/10.1007/978-3-642-28836-4_10.

Sano, Y., Wakita, H., 1985. Geographical distribution of 3He/4He ratios in Japan: implications for arc tectonics and incipient magmatism. J. Geophys. Res. Solid Earth 90 (B10), 8729–8741.

Scarpa, R., Bianco, F., Capuano, P., Castellano, M., D'Auria, L., Di Lieto, B., Romano, P., 2022. Historic Unrest of the Campi Flegrei Caldera, Italy. In: Orsi, G., D'Antonio, M., Civetta, L. (Eds.), Campi Flegrei: A Restless Caldera in a Densely Populated Area. Springer, Berlin Heidelberg, Berlin, Heidelberg, pp. 257–282. https://doi.org/10.1007/978-3-642-37060-1_10.

Selva, J., Orsi, G., Di Vito, M.A., Marzocchi, W., Sandri, L., 2012. Probability hazard map for future vent opening at the Campi Flegrei caldera. Bull. Volcanol. 74 (2), 497–510. https://doi.org/10.1007/s00445-011-0528-2.

Shevenell, L., Goff, F., 1993. Addition of Magmatic Volatiles into the Hot-Spring Waters of Loowit Canyon, Mount St-Helens, Washington, USA. B Volcanol. 55 (7), 489–503. https://doi.org/10.1007/Bf00304592.

Siniscalchi, A., Tripaldi, S., Romano, G., Chiodini, G., Improta, L., Petrillo, Z., D'Auria, L., Caliro, S., Avino, R., 2019. Reservoir structure and hydraulic properties of the Campi Flegrei geothermal system inferred by audiomagnetotelluric, geochemical, and seismicity study. J. Geophys. Res.-Sol. Ea 124 (6), 5336–5356. https://doi.org/10.1029/2018jb016514.

Sorey, M.L., Evans, W.C., Kennedy, B.M., Farrar, C.D., Hainsworth, L.J., Hausback, B., 1998. Carbon dioxide and helium emissions from a reservoir of magmatic gas beneath Mammoth Mountain, California. J. Geophys. Res.-Sol. Ea 103 (B7), 15303–15323. https://doi.org/10.1029/98jb01389.

Stellato, L., Coda, S., Arienzo, M., De Vita, P., Di Rienzo, B., D'Onofrio, A., Ferrara, L., Marzaioli, F., Trifuoggi, M., Allocca, V., 2020. Natural and anthropogenic groundwater contamination in a coastal volcanic-sedimentary aquifer: the case of the archaeological site of Cumae (Phlegraean Fields, Southern Italy). Water 12 (12), 3463. https://doi.org/10.3390/w12123463.

Stimac, J., Goff, F., Goff, C.J., 2015. Chapter 46 - Intrusion-related geothermal systems. In: Sigurdsson, H. (Ed.), The Encyclopedia of Volcanoes, Second edition. Academic Press, Amsterdam, pp. 799–822. https://doi.org/10.1016/B978-0-12-385938-9.00046-8.

Tamburello, G., Caliro, S., Chiodini, G., De Martino, P., Avino, R., Minopoli, C., Carandente, A., Rouwet, D., Aiuppa, A., Costa, A., 2019. Escalating CO2 degassing at the Pisciarelli fumarolic system, and implications for the ongoing Campi Flegrei unrest. J. Volcanol. Geotherm. Res. 384, 151–157. https://doi.org/10.1016/j.jvolgeores.2019.07.005.

Tassi, F., Vaselli, O., Capaccioni, B., Macias, J.L., Nencetti, A., Montegrossi, G., Magro, G., 2003. Chemical composition of fumarolic gases and spring discharges from El Chichon volcano, Mexico: causes and implications of the changes detected over the period 1998-2000. J. Volcanol. Geotherm. Res. 123 (1-2), 105–121. https://doi.org/10.1016/S0377-0273(03)00031-3.

Tedesco, D., 1994. Chemical and isotopic gas emissions at Campi Flegrei: evidence for an aborted period of unrest. J. Geophys. Res. Solid Earth 99 (B8), 15623–15631. https://doi.org/10.1029/94JB00465.

Tedesco, D., Allard, P., Sano, Y., Wakita, H., Pece, R., 1990. Helium-3 in subaerial and submarine fumaroles of Campi Flegrei caldera, Italy. Geochim. Cosmochim. Ac. 54 (4), 1105–1116. https://doi.org/10.1016/0016-7037(90)90442-N.

Tedesco, D., Pece, R., Avino, R., 1996. Radon, pH and temperature monitoring in water wells at Campi Flegrei caldera (southern Italy). Geochem. J. 30 (2), 131–138. https://doi.org/10.2343/geochemj.30.131.

Troiano, A., Di Giuseppe, M.G., Patella, D., Troise, C., De Natale, G., 2014. Electromagnetic outline of the Solfatara-Pisciarelli hydrothermal system, Campi Flegrei (Southern Italy). J. Volcanol. Geotherm. Res. 277, 9–21. https://doi.org/10.1016/j.jvolgeores.2014.03.005.

Valentino, G., Stanzione, D., 2003. Source processes of the thermal waters from the Phlegraean Fields (Naples, Italy) by means of the study of selected minor and trace elements distribution. Chem. Geol. 194 (4), 245–274. https://doi.org/10.1016/S0009-2541(02)00196-1.

Valentino, G.M., Stanzione, D., 2004. Geochemical monitoring of the thermal waters of the Phlegraean Fields. J. Volcanol. Geotherm. Res. 133 (1-4), 261–289. https://doi.org/10.1016/S0377-0273(03)00402-5.

Valentino, G.M., Cortecci, G., Franco, E., Stanzione, D., 1999. Chemical and isotopic compositions of minerals and waters from the Campi Flegrei volcanic system, Naples, Italy. J. Volcanol. Geotherm. Res. 91 (2-4), 329–344. https://doi.org/10.1016/S0377-0273(99)00042-6.

Varekamp, J.C., Ouimette, A.P., Herman, S.W., Bermúdez, A., Delpino, D., 2001. Hydrothermal element fluxes from Copahue, Argentina:: A "beehive" volcano in turmoil. Geology 29 (11), 1059–1062. https://doi.org/10.1130/0091-7613.

Vaselli, O., Tassi, F., Tedesco, D., Poreda, J.R., Caprai, A., 2011. Submarine and inland gas discharges from the Campi Flegrei (Southern Italy) and the Pozzuoli Bay: geochemical clues for a common hydrothermal-magmatic source. Proc. Earth Planet. Sci. 4, 57–73. https://doi.org/10.1016/j.proeps.2011.11.007.

Wigley, T.M.L., Plummer, L.N., Pearson Jr., F.J., 1978. Mass transfer and carbon isotope evolution in natural water systems. Geochim. Cosmochim. Acta 42 (8), 1117–1140. https://doi.org/10.1016/0016-7037(78)90108-4.

Wigley, T.M.L., Plummer, L.N., Pearson Jr., F.J., 1979. Mass transfer and carbon isotope evolution in natural water systems – Errata Corrige. Geochim. Cosmochim. Acta 43, 1395.

Wilhelm, E., Battino, R., Wilcock, R.J., 1977. Low-pressure solubility of gases in liquid water. Chem. Rev. 77 (2), 219–262. https://doi.org/10.1021/cr60306a003.